

# The Effects of Separating Visual and Motor Workspaces on the Generalization of Visuomotor Adaptation across Movement Conditions

Yuming Lei  
*Marquette University*

---

## Recommended Citation

Lei, Yuming, "The Effects of Separating Visual and Motor Workspaces on the Generalization of Visuomotor Adaptation across Movement Conditions" (2013). *Master's Theses (2009 -)*. 214.  
[https://epublications.marquette.edu/theses\\_open/214](https://epublications.marquette.edu/theses_open/214)

**THE EFFECTS OF SEPARATING VISUAL AND MOTOR  
WORKSPACES ON THE GENERALIZATION OF  
VISUOMOTOR ADAPTATION ACROSS  
MOVEMENT CONDITIONS**

by:

Yuming Lei, B.S.

A Thesis submitted to the Faculty of the Graduate School  
Marquette University  
in Partial Fulfillment of the Requirement for  
the Degree of Masters of Science

Milwaukee, Wisconsin

August 2013

**ABSTRACT**  
**THE EFFECTS OF SEPARATING VISUAL AND MOTOR**  
**WORKSPACES ON THE GENERALIZATION OF**  
**VISUOMOTOR ADAPTATION ACROSS**  
**MOVEMENT CONDITIONS**

Yuming Lei, B.S.

Marquette University, 2013

Separating visual and proprioceptive information in terms of workspace locations during reaching movement has been shown to disturb transfer of visuomotor adaptation across the arms. Here, we investigated whether separating visual and motor workspaces would also disturb generalization of visuomotor adaptation across movement conditions within the same arm. In our behavioral study, subjects were divided into four experimental groups (plus three control groups). The first two groups adapted to a visual rotation under a “dissociation” condition in which the targets for reaching movement were presented in midline while their arm performed reaching movement laterally. Following that, they were tested in an “association” condition in which the visual and motor workspaces were combined in midline or laterally. The other two groups first adapted to the rotation in one association condition (medial or lateral), then were tested in the other association condition. The latter groups demonstrated complete transfer from the training to the generalization session, whereas the former groups demonstrated substantially limited transfer. In our fMRI study, we examined brain activity while subjects learned a visuomotor adaptation task in a condition in which visual and motor workspaces were either dissociated or associated with each other, and subsequently performed the same visuomotor task with the same hand in a condition in which visual and motor workspace were associated. Our main results showed that the neural involvement is similar between the early training and the early generalization phases in the ‘dissociation-to-association’ conditions; while that is similar between the late adaptation and the early generalization phases in the ‘association-to-association’ condition. These findings suggest that a visual-proprioceptive conflict in terms of workspace locations disrupts the development of a neural representation, or an internal model, that is associated with novel visuomotor adaptation, thus resulting in limited generalization of visuomotor adaptation.

## ACKNOWLEDGMENTS

Yuming Lei, B.S.

I would like to express my sincere gratitude to Dr. Michelle J. Johnson, my thesis director, for her encouragement and advice. Dr. Johnson has been patient to explain every detail clearly and simply. I will always be grateful for that. I also extremely appreciate Dr. Jinsung Wang for his generous time and valuable advice. Without his assistance this thesis would not have been possible. I thank my thesis committee members, Dr. Kristina Ropella and Dr. Brian D. Schmit for providing their invaluable suggestions to the thesis. I would like to thank Shancheng Bao for his help with fMRI data processing. Finally, I wish to thank my parents, Jianping Lei and Dongjiao Liu for their constant encouragement, inspiration and love.

## TABLE OF CONTENTS

ACKNOWLEDGMENTS .....	i
LIST OF TABLES .....	v
LIST OF FIGURES .....	vi
<b>CHAPTER 1: INTRODUCTION.....</b>	<b>1</b>
1.1 Motor control .....	1
1.2 Sensory prediction .....	2
1.3 Adaptation.....	6
1.4 Motor learning and transfer .....	7
1.5 Neural correlates of motor control.....	9
1.5.1 The primary motor cortex .....	9
1.5.2 The premotor cortex.....	10
1.5.3 The supplementary motor area.....	10
1.5.4 The posterior parietal cortex .....	11
1.6 fMRI.....	12
1.7 Specific Aims.....	12
<b>CHAPTER 2: EXPERIMENTAL EQUIPMENT .....</b>	<b>15</b>
2.1 BKIN Dexterit-E system.....	15
2.1.1 BKIN Dexterit-E system – Calculating hand-based parameters.....	17
2.1.2 BKIN Dexterit-E system – Creating a task program .....	20
2.2 MR-compatible Joystick System Development.....	24
<b>CHAPTER 3: SEPARATION OF VISUAL AND MOTOR WORKSPACES DURING TARGETED REACHING RESULTS IN LIMITED GENERALIZATION OF VISUOMOTOR ADAPTATION.....</b>	<b>28</b>
3.1 Introduction.....	28
3.2 Purpose.....	32
3.3 Material and Methods .....	32
3.3.1 Subject.....	32
3.3.2 Experimental Task .....	32
3.3.3 Experimental sessions.....	34
3.4 Data analysis .....	38

3.5 Results.....	38
3.5.1 Hand-path.....	38
3.5.2 Directional and positional information .....	41
3.5.3 The rate of generalization .....	42
3.6 Discussion.....	44
3.7 Study limitations .....	47
3.8 Conclusion .....	48
<b>CHAPTER 4: BRAIN ACTIVATION ASSOCIATED WITH THE GENERALIZATION OF VISUOMOTOR ADAPTATION: AN FMRI CASE STUDY .....</b>	<b>50</b>
4.1 Introduction.....	50
4.2 Purpose.....	53
4.3 Methods.....	54
4.3.1 Subject.....	55
4.3.2 Experimental Task .....	55
4.3.3 Experimental sessions.....	57
4.3.4 Behavioral data processing .....	59
4.3.5 fMRI acquisition parameters.....	60
4.3.6 fMRI data processing.....	60
4.4 Results.....	63
4.4.1 Behavioral results.....	63
4.4.2 Brain activation observed during the early phase of the training session.....	69
4.4.3 Brain activation observed during the late phase of the training session .....	73
4.4.4 Brain activation during the early phase of the generalization session .....	74
4.5 Discussion.....	78
4.6 Study limitations .....	82
4.7 Conclusion .....	82
<b>CHAPTER 5: CONCLUSION AND FUTURE DIRECTION .....</b>	<b>83</b>
5.1 Conclusion and Future direction.....	83
REFERENCES .....	85
APPENDIX.....	92

APPENDIX A.....	92
APPENDIX B.....	101
APPENDIX C.....	109
APPENDIX D.....	113

**LIST OF TABLES**

3.1: Subject groups .....	35
4.1: Experimental design .....	58
4.2: The first 8 trials in the generalization session in the Dissoc-AssocL condition .....	66
4.3: The first 8 trials in the generalization session in the AssocL-AssocL condition .....	67
4.4: Regions engaged in the dissociation condition.....	70
4.5: Regions engaged in the association-right condition .....	71
4.6: Regions engaged in the association-left condition .....	72

## LIST OF FIGURES

1.1: Sensorimotor transformations formulated in terms of coordinate transformation .....	4
1.2: Forward model.....	5
2.1: Experimental device: KINARM Exoskeleton robots and 2D virtual reality .....	17
2.2: Equations of Motion Parameters .....	19
2.3: A flow chart of task program controls .....	22
2.4: Diagram of MR compatible joystick .....	25
2.5: Connections for MR-joystick .....	26
3.1: Experimental setup of behavioral study .....	33
3.2: Hand-paths from representative subjects in behavioral study .....	38
3.3: Mean performance measures of direction error and final position error .....	40
3.4: Rate of adaptation in generalization session .....	43
4.1: Experimental design of fMRI study .....	56
4.2: Schematic diagram of VMAL, VMD and VMAR .....	59
4.3: Hand-paths from representative subjects in fMRI study .....	64
4.4: Performance measures of direction error and endpoint error during the training session.....	68
4.5: Performance measures of direction error and endpoint error during the generalization session .....	69
4.6: Brain activations during the early phase of the training session.....	73
4.7: Brain activations during the late phase of the training session.....	75
4.8: Brain activations during the early phase of the generalization session for the dissociation conditions .....	75
4.9: Brain activations during the early phase of the generalization session for association condition .....	76
4.10: Activation patterns across the early, late phase of the training sessions and the early phase of the generalization session for the association condition .....	77
4.11: Activation patterns across the early, late phase of the training sessions and the early phase of the generalization session for the dissociation condition .....	78

## **Chapter 1**

### **Introduction**

In this thesis, I investigated the pattern of visuomotor adaptation during targeted reaching movement and examined the effect of separating visual and motor workspaces on the neural representations that underlie the visuomotor adaptation. In this chapter, I present background research that has set the foundation for this thesis, which includes the following topics: motor control, sensory prediction, adaptation, motor learning and transfer, neural correlates of motor control, and functional MRI (fMRI). The specific aims of this thesis are presented at the end of this chapter.

#### **1.1 Motor control**

Motor control is a study within neuroscience of how organisms control volitional and reflexive movements. Here we focus on goal-directed volitional movement. Goal-directed movements are carried out to accomplish a specific goal. The control of goal-directed movement is complex. Voluntary behaviors, such as an eye movement or an arm movement, may recruit many neurons and use many parts of the brain. Considering a goal-directed reaching movement, for example, visual information about a target is processed in the visual cortex to identify the location of the target and compute the direction and velocity of the hand movement; and proprioceptive information from the parietal lobe that is related to the position of the arm in three-dimensional space is also computed by the brain to plan the movement. All sensory information ultimately reaches multisensory processing regions in the cerebral cortex called association areas. The association areas make connections with higher-order motor centers that compute a motor

command for moving the hands into a desired position. This motor command is then passed on to the motor cortex to activate the correct muscles in the shoulder, arm, and hand to complete the movement. Voluntary movements differ from reflexive movements in three ways: (1) voluntary movements are planned for purposeful tasks, therefore the selection of joints and body segments depends on the goal of the given behavioral task; (2) voluntary movements can improve with learning; and (3) voluntary movements are generated internally rather than through environmental stimuli.

## **1.2 Sensory prediction**

Sensorimotor transformation refers to a process in which sensory signals are converted into a motor command to generate a movement. A typical example of such transformation is to reach for a target currently in view with the hand. In this case, two issues must be resolved (Cunningham and Welch 1994; Kawato 1999; Kawato et al. 1988, 1990; Krakauer et al. 1999, 2000; Rosenbaum and Chaiken 2001): (1) specification of movement kinematics: where a desired hand position relative to the location of the target is determined; and (2) specification of movement dynamics, where the appropriate muscle forces are specified to carry out the desired movement trajectory. In this study, we focus on the kinematics specification of reaching movement.

Sensorimotor transformations are often formulated in terms of coordinate transformation, in which the target position is encoded in the eye-centered (retinal) coordinate in the early stages of motor planning; and the hand position is encoded in the eye-centered coordinate, body-centered coordinate, or both. It is widely accepted that the nervous system represents and plans a reaching movement in terms of a vector in extrinsic space in which its extent and direction are specified (Vindras and Viviani 1998;

Krakauer et al. 2000). To reach for a target such as a coffee cup while fixating on a newspaper, for example, the spatial position of the cup is initially represented in the brain from the eye-centered coordinate; the position of the hand is represented in the brain in terms of its location in the body-centered coordinate. In order to reach for the cup, the central nervous system (CNS) needs to compute the difference between the target location and the current location of the hand. Figure 1.1 denotes the target location and the hand location as  $X_t$  and  $X_{ee}$ , respectively. The difference between these two vectors represents the desired difference vector ( $X_{dv}$ ). The CNS transforms the desired difference vector into a trajectory with a specific kinematic plan, and then computes the specific forces needed to transform this trajectory from a kinematic plan into an action.

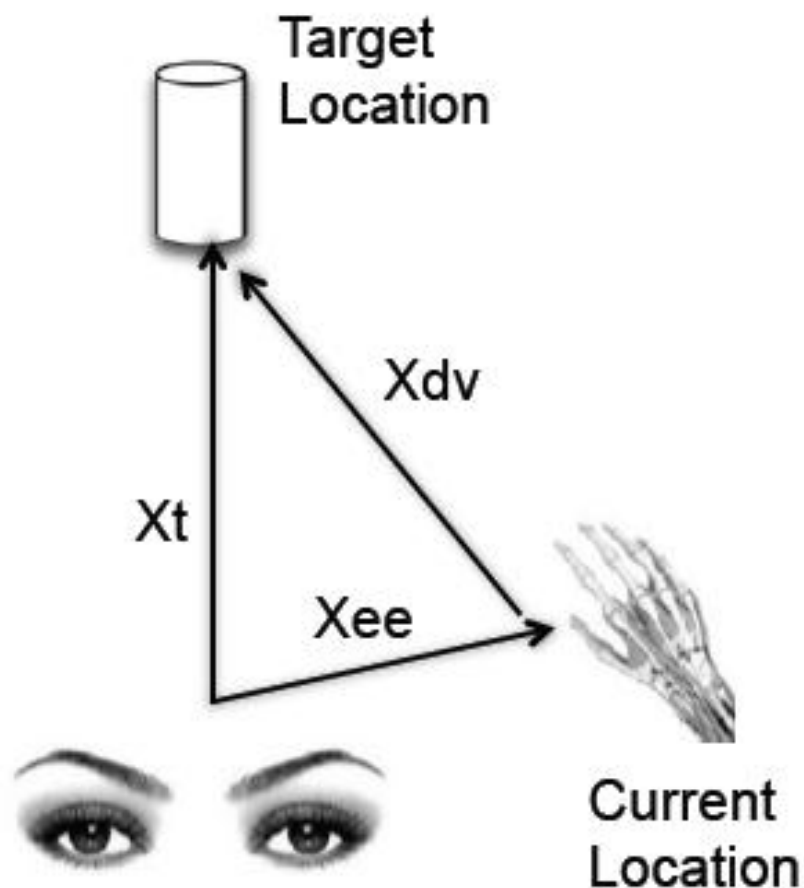


Figure.1.1, Target location is specified in retinal-centered coordinate with vector  $X_t$ ; Hand location is specified in body-centered coordinate with vector  $X_{ee}$ ; the difference vector  $X_{dv}$  is the distance and direction that the hand must move to reach the target.

Although the target location must be detected by vision, the end-effector location may depend on other sensory information. In terms of goal-directed reaching movement with arm, the location of the hand can be determined by visual and/or proprioceptive information about the hand. Visual information includes the retinal location of the hand, while proprioceptive information includes information associated with the configuration and orientation of the hand, head, and eyes. Consider a scenario in which one reaches for

a coin that is in the water. In order to reach for the coin accurately, the motor system needs to take into account for the changes in the environment (i.e., the mismatch between the actual location of the coin and the coin position sensed through his/her eye) when planning the reaching movement. The solution to this problem is a forward model (Fig 1.2).

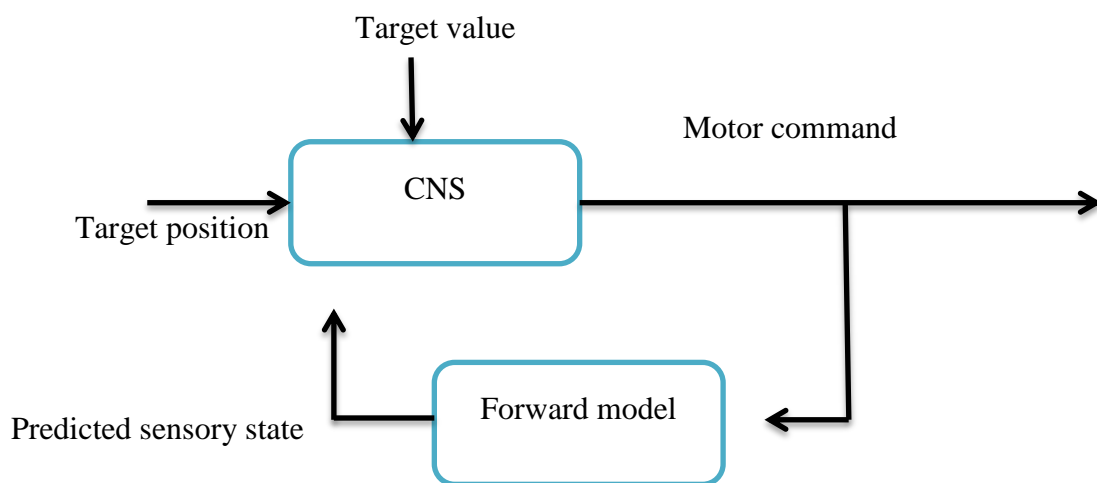


Figure.1.2, Forward model receives a copy of motor command and generates a predicted sensory state at a short latency. The predicted sensory consequence is integrated with true sensory feedback to optimize state estimate.

Goal-directed reaching movement relies on the forward model that would enable the nervous system to predict state variable such as position and direction based on a history of motor commands (Ariff et al. 2002, Mehta and Schaal 2002, Flanagan et al. 2003) and to generate a motor command based on our estimate of current limb position. Let's return to our previous example that one plans to reach for a coin placed in the water. If s/he reaches for the coin for the very first time, the brain will plan a desired hand

location at the end of reaching movement based on the visual information of the coin location. In this case, the motor command will reflect a predicted limb state. However, the movement planned based on this predicted state will not result in a successful performance because the predicted limb state was based on a distorted visual estimate of the coin location. When s/he reaches for the coin for the second time, the forward model will receive a copy of a motor command from the previous movement and generate a newly predicted limb state. This newly predicted state is integrated or updated with sensory feedback from the previous movement to provide corrections to the movement error caused by distorted visual information of the coin location.

It appears that our brain combines what it had predicted for previous actions with the sensory feedback that corresponds to current actions, and adapts an internal representation of the relationship between the limb state and the environment (called 'internal model'), which is then used by the brain to guide future actions. If a prediction made by the internal model results in an accurate movement outcome, the internal model is maintained in a stable state. However, a movement results in some prediction error due to an unexpected perturbation, the internal model starts a calibration process based on currently available information until the prediction errors are minimized. By doing so, the internal model can allow one to perform a reach movement even under an altered visual-motor environment (e.g., reach for a coin placed in the water).

### **1.3 Adaptation**

Humans have a remarkable capability to adapt and modify motor behavior in response to any changes in the body and the environment. Maintaining a desired motor behavior may be achieved through adaptation of an internal model that predicts the

sensory consequence of motor commands (Shadmehr et al. 2010). There are two general types of adaptation paradigms that involve arm movements: visuomotor adaptation and force-field adaptation. Here we focus on the visuomotor adaptation paradigm. Visuomotor adaptation has served as a well-established paradigm for studying the capability of the CNS that copes with altered visual feedback (Abeele and Bock 2001a, 2001b, 2003; Imamizu and Shimojo 1995; Krakauer et al. 2000). Typically, the main paradigm is to distort visual information about initial hand position by the use of either optical prisms or virtual reality environments. For example, in a visuomotor adaptation study conducted in 1867 by Hermann von Helmholtz, subjects who made pointing movement toward targets while wearing prism lenses that displaced the visual field laterally initially experienced leftward direction errors during pointing movements, but could compensate for the errors after some practice. As soon as the prisms were removed, they made rightward direction errors (called ‘after-effect’). After-effect is considered strong evidence that a new internal model has been developed as a result of sensorimotor adaptation.

#### **1.4 Motor learning and transfer**

Visuomotor adaptation is one category of motor learning. Another important question associated with visuomotor adaptation is how much an internal model developed in one movement condition can be generalized to another movement condition. A large number of studies make use of a transfer test to determine the generalizability of an internal model. Generalization of motor learning refers to the degree to which a given internal model can be effectively used across motor tasks, workspaces, effectors, and limb configurations. The patterns of generalization or transfer could be used to infer

whether an internal model is task specific condition specific, etc. For example, if one is an expert in the game of table tennis, and now s/he is going to learn tennis, can s/he apply what s/he has learned from table tennis to playing tennis? In the rehabilitation domain, can a rehabilitative training received under a specific physical therapy setting transfer to facilitate movement under an unconstrained environment? These questions can be addressed by studying the transfer of motor learning.

A large number of studies have investigated the mechanisms underlying the transfer of visuomotor adaptation. Baraduc and Wolpert (2002), for example, conducted a study to investigate how local changes in the displacement map affected the movement that started in the same location, but had different initial arm configuration. In that study, they found that the internal model of the map from hand location to joint displacement affect the mapping for those “untrained” postures, indicating an internal model generated in one arm configuration can generalize to other arm configurations. Some studies indicated that visuomotor remapping is not restricted to the workspace in which adaptation took place, which suggests that the internal model of visuomotor adaptation can generalize across different workspaces (Heuer et al. 2011; Krakauer et al. 2000; Wang et al. 2005). The previous studies in our lab showed that visuomotor adaptation can also transfer from one arm to the other. Wang and colleagues (2002, 2006), for example, reported that when subjects adapted to a rotated visual display with one arm first, then with the other arm, directional information of reaching movement transfers primarily from the non-dominant to the dominant arm, whereas positional information transfers primarily from the dominant to the non-dominant arm. This suggests that the internal

model developed during visuomotor adaptation can generalize across different motor effectors (i.e., arms).

## **1.5 Neural correlates of motor control**

Goal-directed movement is organized in the cerebral cortex. The motor areas of the cerebral cortex associated with voluntary movement control include the primary motor cortex and several premotor areas. Each motor area contains large neurons that send long axons down the brain stem and spinal cord to synapse on the interneuron circuitry of the spinal cord and also directly on the alpha motor neurons in the spinal cord which connect to the muscles.

### **1.5.1 The primary motor cortex**

The primary motor cortex (M1) contains a rough motor map of control areas for the face, digits, hand, arm, trunk, leg, and foot in an orderly arrangement along the gyrus. Therefore, M1 is regarded as the main contributor to generating neural impulses that pass down to the spinal cord and control the execution of movement. Evarts (1968) suggested that once a neuron in M1 becomes active, it projects to the spinal cord in which the signal is relayed to the alpha motor neuron that connects to the muscles. Some studies (Scott et al. 1995; Moran et al. 1999; Kakei et al. 1999) also found that some neurons in motor cortex are associated with muscle forces and others with the spatial direction of movement. However, which neurons in M1 control the spinal cord, and thus movement, remains to be further investigated.

### **1.5.2 The premotor cortex**

Unlike the M1 in which neurons are thought to be primarily involved in controlling simple movements of single joint, neurons in the premotor cortex (PM) often are responsible for more complex movements involving multiple joints. The PM is also in association with some aspects of motor control, including the preparation for movement, the sensory guidance of movement and the spatial guidance of reaching. Recent anatomical studies (Graziano et al 2008; Matelli et al 1985; Preuss et al 1996) indicated the premotor cortex is divided into four main areas including PMDc (premotor dorsal, caudal), PMDr (premotor dorsal, rostral), PMVc (premotor ventral, caudal) and PMVr (premotor ventral, rostral). The role of PMDc is associated with guiding reaching (Hoehrmann et al 1991; Churchland et al 2006); PMDr participates in learning to associate sensory stimuli with specific movement (Weinrich et al 1984; Brasted et al 2004; Muhammad et al 2006); PMVc is related to the sensory guidance of movement (Rizzolatti et al 1981; Fogassi et al 1996; Graziano et al 1994; Graziano et al 1999); and PMVr relates to shape the hand during grasping (Rizzolatti et al 1988); These premotor areas project to both the M1 and the spinal cortex, with fewer projections to the spinal cord than to the M1.

### **1.5.3 The supplementary motor area**

The supplementary motor area (SMA) locates on the top or dorsal part of the cortex. It is known that each neuron in the SMA may influence many muscles and the two sides of the body, therefore SMA can project directly to the spinal cord or play some direct role in movement control (Gould et al 1996; Luppino et al 1991; Mitz et al 1987;). Since the direction projection of SMA to the spinal cord and its activity during simple movements, SMA is considered to play a direct role in motor control rather than a high level role in planning sequences (Picard et al 2003). Imaging studies also suggested that stimulation of the SMA can give rise to bilateral movements, indicating that this area may play a role in coordinating movements on both sides of the body (Brinkman 1981).

### **1.5.4 The posterior parietal cortex**

In addition to the motor cortices, the posterior parietal cortex (PPC) also plays an important role in voluntary movements. Each PPC area is involved in the analysis of particular aspects of sensory information, including visual, proprioceptive and auditory information. Before an effective voluntary movement can be initiated, the PPC must receive visual, proprioceptive and auditory inputs to determine the location of the body and external objects in space, therefore it generates internal representation of the movement to be made, prior to the involvement of the motor cortices. The output of the PPC goes to areas of frontal motor cortex. Damage to PPC can result in a variety of sensorimotor deficits, including difficulty reaching to a visual target in the absence of specific visual or motor deficits (Pinel et al 2007).

## **1.6 fMRI**

A variety of brain imaging tools have been developed to examine the neural correlates of brain activity within the last decades, including functional magnetic resonance imaging (fMRI), positron emission tomography (PET), and near infra-red spectroscopy (NIRS), etc. fMRI is a non-invasive imaging technique that measures neural activity relying on the fact that brain activation and cerebral blood flow are coupled. When a brain region involved in a given task, process or emotion is active, it causes oxygen and glucose consumption, which results in an increased blood flow to the neighborhood region. As more oxygenated hemoglobins are delivered to the neighborhood region of activated neurons, the density of deoxygenated hemoglobin decrease; and as a result, the blood oxygenated level dependent (BOLD) signal increases. fMRI utilizes the magnetic properties of blood to reflect the neuron activation, and fMRI images are reconstructed from the BOLD signal that is associated with the metabolic activity neurons. In this study, we use fMRI to map the cortical representation of visuomotor adaptation during reaching movement. An fMRI-compatible joystick system was used to control record and evaluate reaching movement.

## **1.7 Specific Aims**

In general, I investigated the development of an internal model following adaptation to a novel visual rotation during targeted-reaching movement in this study. The overall objective of this study was to understand the contributions of visual and proprioceptive information to the development of neural representations that underlie

adaptation to a novel visuomotor transformation. This objective was achieved by pursuing the following two specific aims:

**Aim 1:** To examine how visual and proprioceptive information associated with workspace locations during targeted reaching movement contributes differentially to the development of internal models underlying novel visuomotor adaptation (experiment 1, described in chapter 3).

**Aim 2:** To develop and confirm an fMRI technique to investigate the neural representations involved in the differential contributions of visual and proprioceptive information to the development of internal models underlying novel visuomotor adaptation (experiment 2, described in chapter 4).

Findings from this research will lead to a better understanding of the neural mechanisms that underlie sensorimotor learning. Given that generalization of motor learning across different movement conditions or environments is important for neuro-rehabilitation (Krakauer, 2006), investigations of the neural processes underlying sensorimotor adaptation may prove valuable for the development of more efficient rehabilitation protocols for individuals who lost motor function due to various neuromotor problems such as stroke.

The remainder of thesis is outlined as follows: Chapter 2 describes the experimental equipment used in the two experiments conducted. Chapter 3 describes the behavioral experiment used to determine the impact of dissociation or association of

visual and proprioceptive information in terms of workspace on internal model building (Aim 1). Chapter 4 describes a case study investigating the neural substrates underlying the visual and proprioceptive workspaces dissociation/association in visuomotor adaptation (Aim 2). The techniques were developed to replicate key aspects of the behavioral experiment in Chapter 3 to provide insight into the neural process sub-serving the adaptation observed. Finally, Chapter 5 describes major contributions and future directions.

## **Chapter 2**

### **Experimental Equipment**

In this chapter, I described two pieces of equipment that were used in this study: BKIN Dexterit-E system and MR-compatible joystick system. The former system was used to collect kinematic data during goal-directed reaching movement in experiment 1 (chapter 3), whereas the latter system was used to collect kinematic data in the MR environment in experiment 2 (chapter 4). Each of the two systems is described in the following section.

#### **2.1 BKIN Dexterit-E system**

The BKIN Dexterit-E system (BKIN Technologies Ltd, Kingston, ON, Canada) was used to collect kinematic data in our behavioral study, which consists of two KINARM Exoskeleton robots for the upper limbs, a 2D virtual reality display and Dexterit-E<sup>TM</sup> experimental control and data acquisition software (Fig 2.1.A). Each KINARM robot can be used as an exoskeleton for each arm; and the 2D virtual reality display is used to present visual stimuli in such a way that the stimuli (e.g., targets for reaching movements) appear at the same horizontal level as the hand (Fig 2.1.B). Dexterit-E<sup>TM</sup> experimental control and data acquisition software are designed to run on a multi-computer system. Dexterit-E itself runs on a Windows-based computer, in which it effectively acts as a user-interface for choosing task protocols, providing visual feedback to the operator, and saving data. The chosen task protocol is associated with a real-time computer, which is used to control the task. The real-time computer runs an operating system from the Mathworks Corporation called xPC Target. During the execution of a

task, the communication from the real-time computer to the Windows-based computer allows the Windows-based computer to offer online feedback to the operator.

The KINARM robot is a motorized exoskeleton for the arm that allows manipulation of the arm in the horizontal plane. The KINARM's joints are aligned with the subject's shoulder and elbow joints. Therefore, subject does not experience the KINARM inertia adversely. Position feedback is acquired through incremental encoders that are integral to the motors, with a feedback resolution of 20,000 per revolution at the motor, which at the joint angles is equal to 80,000 per revolution because of the 4x gear ratio in the KINARM robot.

A



B

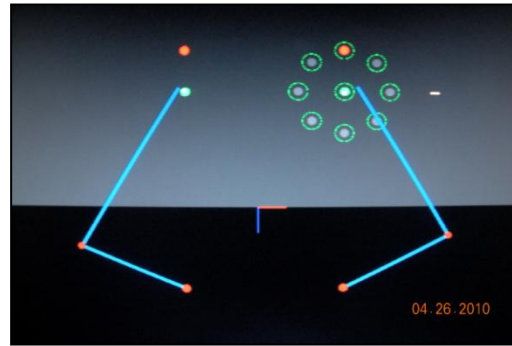
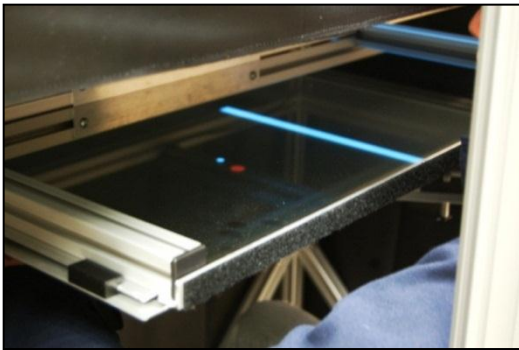


Figure.2.1, Experimental device. A: KINARM Exoskeleton robots. B: 2D virtual reality

### 2.1.1 BKIN Dexter-E system – Calculating hand-based parameters

BKIN Dexter-E data is stored largely in a joint-based format. Figure 2.2 shows the kinematic setup of the KINARM robot. The kinematics of human arm refers to the relationship between hand positions and joint positions and transformation between these two coordinate systems. To convert to end-point coordinates (i.e. hand or finger-tip

based), we used the forward kinematic equation to determine the position and orientation of the end-effectors, given the values for the joint variables. The following equations are used to describe position, velocity and acceleration:

$$X_{Hand} = X_{Sh} + L_1 \cos \theta_1 + L_2 \cos \theta_2 + L_{ptranterior} \cos \theta_{2ptr} \quad \text{Eq. 2.1}$$

$$Y_{Hand} = Y_{Sh} + L_1 \sin \theta_1 + L_2 \sin \theta_2 + L_{ptranterior} \sin \theta_{2ptr} \quad \text{Eq. 2.2}$$

$$\dot{X}_{Hand} = -L_1 \sin(\theta_1) \dot{\theta}_1 - L_2 \sin(\theta_2) \dot{\theta}_2 - L_{ptranterior} \sin(\theta_{2ptr}) \dot{\theta}_2 \quad \text{Eq. 2.3}$$

$$\dot{Y}_{Hand} = L_1 \cos(\theta_1) \dot{\theta}_1 + L_2 \cos(\theta_2) \dot{\theta}_2 + L_{ptranterior} \cos(\theta_{2ptr}) \dot{\theta}_2 \quad \text{Eq. 2.4}$$

$$\ddot{X}_{Hand} = -L_1(\cos(\theta_1) \dot{\theta}_1^2 + \sin(\theta_1) \ddot{\theta}_1) - L_2(\cos(\theta_2) \dot{\theta}_2^2 + \sin(\theta_2) \ddot{\theta}_2) - L_{ptranterior}(\cos(\theta_{2ptr}) \dot{\theta}_2^2 + \sin(\theta_{2ptr}) \ddot{\theta}_2)$$

Eq. 2.5

$$\ddot{Y}_{Hand} = L_1(-\sin(\theta_1) \dot{\theta}_1^2 + \cos(\theta_1) \ddot{\theta}_1) - L_2(-\sin(\theta_2) \dot{\theta}_2^2 + \cos(\theta_2) \ddot{\theta}_2) + L_{ptranterior}(-\sin(\theta_{2ptr}) \dot{\theta}_2^2 + \cos(\theta_{2ptr}) \ddot{\theta}_2)$$

Eq. 2.6

$X_{Sh}$  – X coordinate of shoulder axis

$Y_{Sh}$  – Y coordinate of shoulder axis

$L_{ptranterior}$  – Anterior position of fingertip relative to long axis of L2 segment

$\theta_{2ptr}$  – Perpendicular angle from long axis of L2 segment to fingertip, defined in a right-handed global coordinate system.

$L_i$  – Inter-joint length of the  $i^{\text{th}}$  segment. The length referred to here is the robot segment length.

$\theta_i$  – Angle of  $i^{\text{th}}$  segment defined in a global coordinate system.

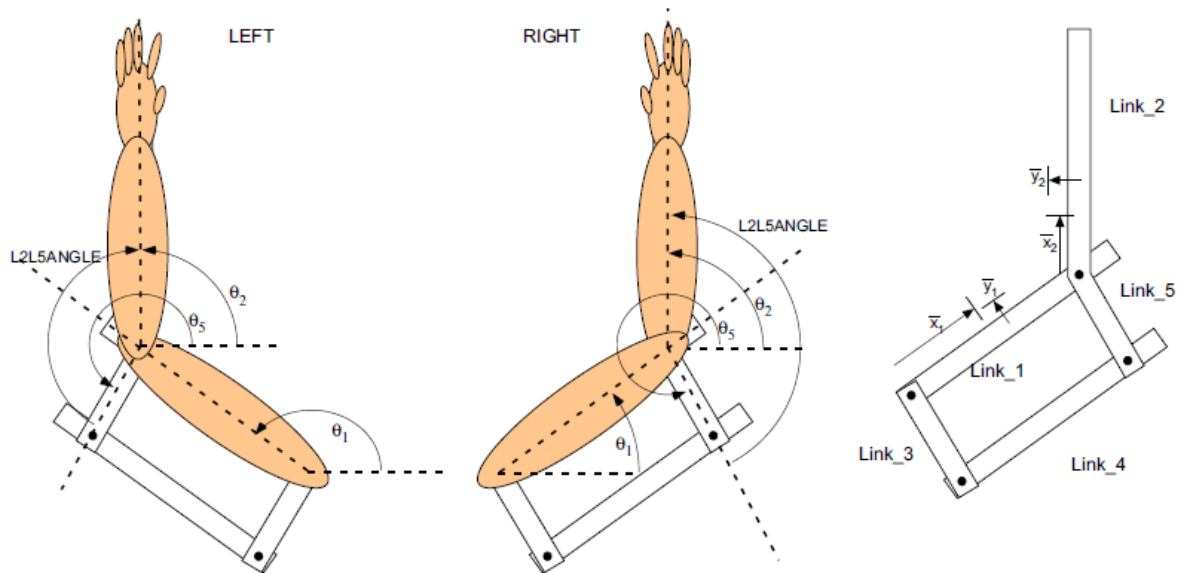


Figure 2.2, Equations of Motion Parameters

In this study, we had 35 subjects showing the average upper arm length (L1) 57.65cm and the average forearm length (L2) 45.69cm.

### 2.1.2 BKIN Dexterit-E system – Creating a task program

Task programs are created to define and control the system behavior that can occur during a single trial of a task in BKIN Dexterit-E system. For a general class of point-to-point reaching tasks, the task program could be defined as follows:

1. A target will turn on during a trial.
2. Once a subject reaches to that target, it will turn off and another target will turn on.
3. The subject reaches to the second target, which will turn off at the end of reaching movement.
4. The trial is over.

The task program does not define the details of the task, such as the target location, color and number of trials. These parameters are specified through the BKIN Dexterit-E's windows-based user interface. Programming a task program involves Simulink and Stateflow toolboxes. Simulink is a block diagram environment for a model-based design in which task programs are developed and represented as a graph of data flow in the task. Stateflow is a graphical design tool for developing event-driven state machine that allows transitions between the states defined in the task. Task programs are built by Matlab and xPC Target toolbox using a third party C/C++ compiler.

The figure below shows a flow chart that happens during a single trial of the task in our study. In this flow chart, states are represented by ovals and transitions between states are represented with arrows. An event can only exist in one state at a time, and the event must be in one of the defined states. The event transfer from one state to another

can only occur when there is a transition between the states, and the conditions for that transition are true.

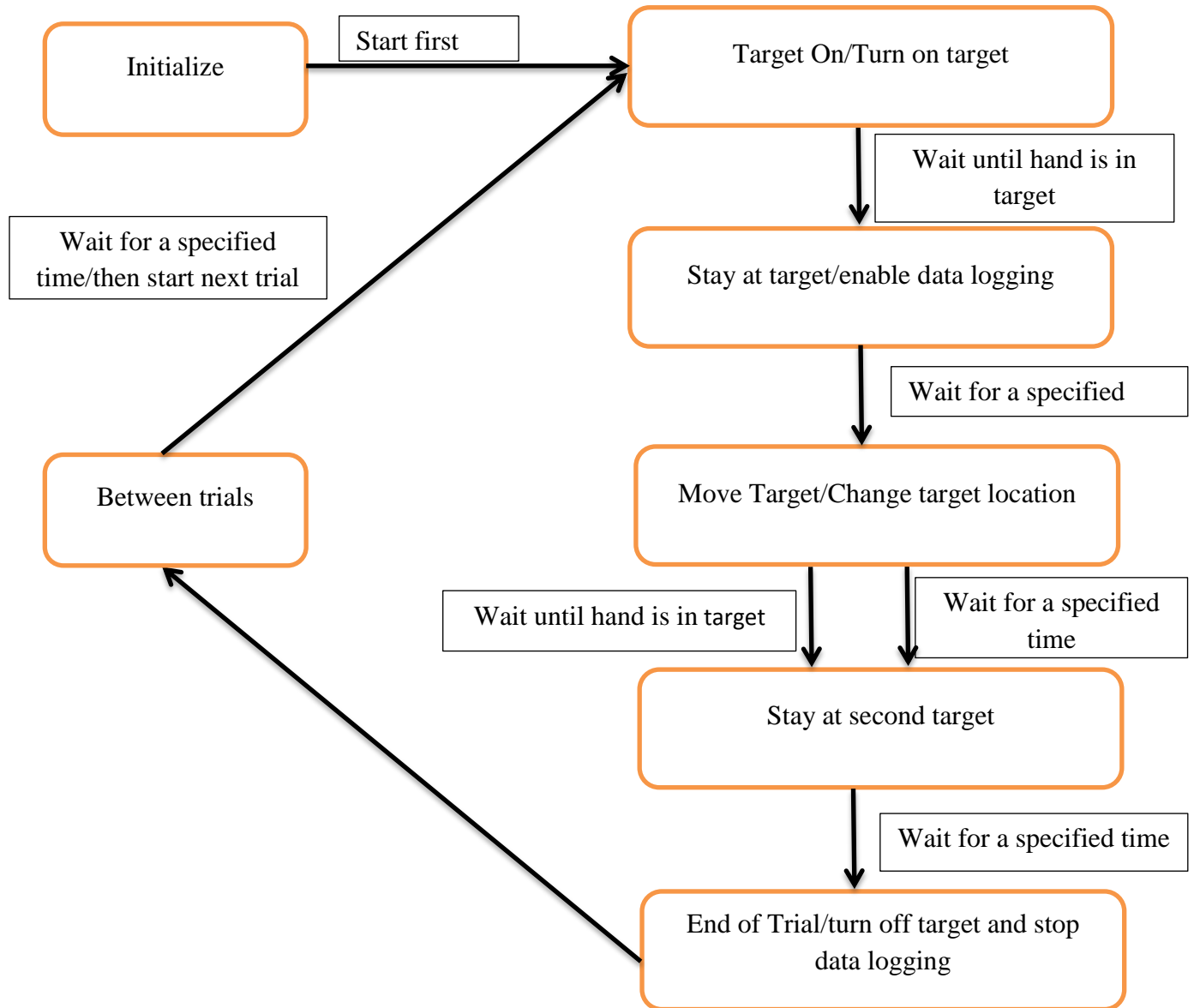


Figure 2.3, A flow chart of task program controls

Below shows seven states in the flow state:

**Initialize** – When this state is entered, the task program will begin. There are no conditions for the transition leading to the Target on state, so the system immediately switches to the Target on state.

**Target On** – When this state is entered, the first target will be turned on. The event will stay in this state until the condition “wait until hand is in target” is true.

**Stay At First Target** – When this state is entered, data logging is initialized. Once the condition “wait for a specific time” is true, the event will switch to the “Move Target” state.

**Move Target** – When this state is entered, the target will be moved to the peripheral position. There are two possible conditions for exiting in this state (if either is true, then the transition will occur): (1) the event will switch to the “Stay At Second Target” if the condition “wait until hand is in target” is true. (2) Once a specified period of time has elapsed, the event will switch to the “Stay At Second Target”. If either is true, then the transition will occur.

**Stay At Second Target** – When this state is entered, nothing happens. Once the condition “wait for a specific time” is true, the event will switch to the “End Of Trial” state.

**End Of Trial** – When this state is entered, the target will be turned off. This state will switch to “Between Trials” state. There is no condition on this transition, so it occurs immediately.

**Between Trials** – When this state is entered, State flow sends a signal to the task program that trial is over and to provide a specific time delay, allowing the Task Program to update the Trial Protocol for the next trial. Exiting from this state back to the “Target On state” for the next trial occurs after a specified time delay.

## **2.2 MR-compatible Joystick System Development**

The MR-compatible joystick system consists of a commercial joystick with integrated cable, a USB interface box and behavioral control and data acquisition software called MovAlyzeR (NeuroScript, Tempe, AZ). In general, a MR-compatible device should not contain ferrous material, because ferrous object might be lifted up or pulled away inside a strong magnetic field, resulting in human injury or equipment damage. In addition, any conductive or dielectric material should be excluded from the device material, because those materials could distort the magnetic field. The joystick used in our study contains no ferromagnetic parts, which avoids interference with scanner operation. This joystick is commercial available (Fig 2.4) (Mag Design and Engineering) and its MR compatibility has been tested elsewhere.



Figure 2.4, Diagram of MR compatible joystick.

The USB interface does not require an AC power adapter to be connected, and it can be connected or disconnected from the computer at any time. The joystick appears in the list of the computer if USB interface box is connected; double clicking on the joystick listing and the cursor appears showing the joystick's position. Figure 2.5 shows the connections for MR-joystick.

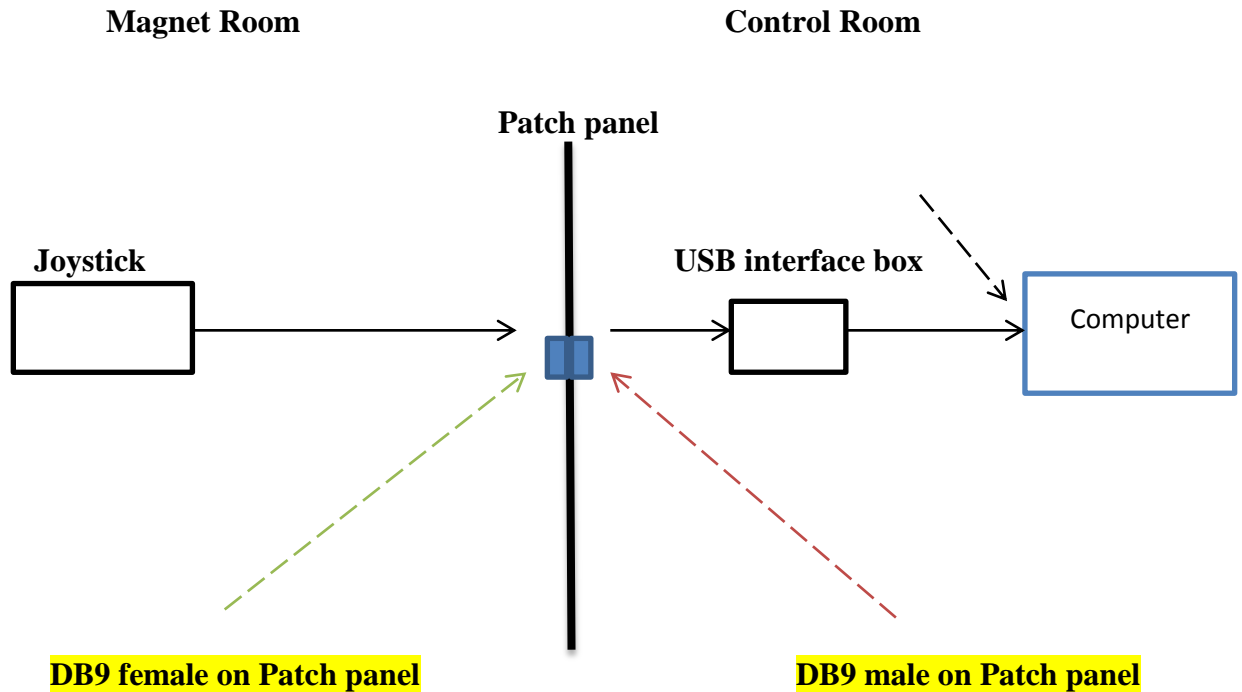


Figure 2.5, Connections for MR-joystick

The MovAlyzeR is a software package that was originally developed for handwriting research. Here, it is used for joystick-movement test in our fMRI study. This software enabled us to present targets for reaching movement and also to collect data during movement performed with MR-compatible joystick. MovAlyzeR has a simple user interface for running movement tests, which also includes the stimulus editor companion program for accurately designing visual stimuli to display. We developed a

visuomotor adaptation task with MovAlyzeR that required subjects to use a joystick to move a screen cursor to the targets. In the Kinarm set-up, a complex visuomotor coordinate transformation task involving goal-directed arm movements had to be performed by the subjects, requiring shoulder flexion, elbow extension, and wrist pronation or supination. In the MR scanner set-up, the movements associated with the use of the joystick consisted of rotation and translation of the right wrist and the forearm, and to a small degree rotation in the shoulder joint while the finger rested on the shaft of the joystick. Neural activities are more associated with the task rather than the use of the end-effector in motor learning, so similar neural activities should be involved for point-point reaching movement even for these two different experiment set-ups.

## Chapter 3<sup>1</sup>

### **Separation of visual and motor workspaces during targeted reaching results in limited generalization of visuomotor adaptation**

#### **3.1 Introduction**

It is generally accepted that vision and proprioception are both critical to effective motor control and learning. When carrying out goal-directed movement in a given environment, at least three serially organized processes are thought to happen (Cunningham and Welch 1994; Jordan and Rumelhart 1992; Kawato 1999; Kawato et al. 1988, 1990; Krakauer et al. 1999, 2000; Rosenbaum and Chaiken 2001; Sainburg 2002): (1) Visual information about the target location is transformed into an internal reference frame, whose process is defined as a “visuomotor map” of the relationship between extrinsic visual coordinates and intrinsic motor commands; (2) Trajectory specification, where desired body positions are specified in terms of movement trajectory; and (3) Dynamic specification, where the appropriate muscle forces are specified to carry out the desired movement trajectory. The role of visual information in these processes is largely associated with the external environment, as the motor control system adjusts to changes and unexpected perturbations in the external environment through visual feedback. The major role proprioceptive information plays in these processes is in the planning and modification of internal motor commands as proprioception provides information regarding position and muscle forces to the motor control system (Bagesteiro et al. 2006).

---

<sup>1</sup> Lei, Y., Johnson, M. J., & Wang, J. (2013). Separation of visual and motor workspaces during targeted reaching results in limited generalization of visuomotor adaptation. *Neuroscience Letters*, Epub ahead of print.

A number of researchers investigated the involvement of visual and proprioceptive information in controlling voluntary reaching movement and suggested that they play differential roles in the planning and execution of reaching movement (e.g., Redding and Wallace 1996; Goodbody and Wolpert 1999; Sainburg 2005; Sainburg et al. 2003). For example, Sainburg and colleagues suggested that vision plays a more important role for planning movement trajectories while proprioception is more important for online correction of movement (Sainburg et al. 2003; Bagesteiro et al. 2006) This is in agreement with the idea that visual and proprioceptive information may be combined in fundamentally different ways during trajectory control and final position control (Scheidt et al. 2005). It has been further suggested that vision and proprioception play a weighted role in targeted reaching movement in such a way that the brain weighs the two types of sensory inputs relatively depending on the sensory modality of the target and on the information content of the visual feedback (Sober and Sabes 2005). These findings collectively indicate that the contributions of visual and proprioceptive information to the control of voluntary movement may vary throughout the movement, that is, from its planning to its execution. Although both vision and proprioception are known to be essential for performing an accurate movement, not much is known regarding the effect of visual and proprioceptive information on the development of an internal model following adaptation to a novel visual rotation.

To understand the nature of visuomotor adaptation, various types of experimental paradigms have been used, one of which involves examining the influence that workspaces have on the pattern of visuomotor adaptation and its generalization (Heuer et al. 2011; Krakauer et al. 2000; Thomas et al. 2012; Vetter et al. 1999; Wang et al. 2005).

Some studies demonstrated extensive generalization of visuomotor adaptation across different workspaces, indicating that visuomotor remapping is not restricted to the workspace in which adaptation took place (Heuer et al. 2011; Krakauer et al. 2000; Vetter et al. 1999; Wang et al. 2005). Other studies, however, demonstrated that individuals can adapt to conflicting visuomotor conditions simultaneously when the conditions are associated with different workspaces (Thomas et al. 2012; Woolley et al. 2007), suggesting that visuomotor remapping associated with a given condition can be localized to a specific workspace in which adaptation occurred. Given the two sets of findings that seemingly contradict each other, more research is needed to better understand the effect of workspaces on the pattern of visuomotor adaptation and its generalization.

In the aforementioned studies, generalization of visuomotor adaptation was examined across workspaces in which the same arm performed reaching movement. The effect of workspaces has also been examined in interlimb transfer studies, in which the workspaces where the two arms performed motor tasks were either combined or separated (Krakauer et al. 2000, Woolley et al. 2007). Sainburg and Wang (2002) had subjects adapt to a rotated visual display with the dominant arm first, then with the nondominant arm, or vice versa, and observed that directional information of reaching movement only transferred from the nondominant to dominant arm. In that study, both arms adapted to the rotation in a shared midline workspace. In a follow-up study in which each arm adapted to the same rotation in a separate lateral workspace (Wang et al. 2006), directional information transferred in both directions (i.e., dominant to nondominant arm, and vice versa), indicating that the pattern of interlimb transfer depends on the workspace locations in which the arms adapt to visual rotations.

More recently, Wang (2008) showed that interlimb transfer of directional information did not occur at all when visual and motor workspaces were separated during visuomotor adaptation (e.g., targets were displayed in a shared midline workspace while each arm physically performed the task in its ipsilateral workspace). This finding may indicate that a conflict between visual and proprioceptive information in terms of workspace locations inhibits the access of each arm controller to the movement information obtained by its counterpart, probably due to uncertainties in determining hand dominance at a given workspace. Alternatively, such a conflict may lead to incomplete development of a neural representation associated with the given visuomotor condition. These two interpretations lead to different predictions: the former predicts that a conflict between visual and motor workspaces should not interfere with generalization of visuomotor adaptation across movement conditions in which the same arm is used, whereas the latter predicts that it should. In the latter case, generalization across the arms should be minimal as well, because the neural representation developed during the initial training phase was incomplete in the first place.

## **3.2 Purpose**

In the present study, thus, we separated visual and motor workspaces during visuomotor adaptation to examine how the adaptation would generalize across different conditions that involved the same arm movement.

## **3.3 Material and Methods**

### **3.3.1 Subject**

Subjects were 35 neurologically intact young adults, ranging from 18 to 30 years. All subjects were right handed. Handedness of the subjects was determined using the 10-item version of Edinburgh Handedness Inventory (Oldfield 1971). Subjects were paid for their participation. Informed consent approved by the institutional Review Boards of the Marquette University and the University of Wisconsin-Milwaukee, was solicited prior to participation. Subjects were randomly assigned to one of seven groups (5 subjects per group).

### **3.3.2 Experimental Task**

Subjects were seated on a height-adjustable chair facing a table with the right arm supported on the exoskeleton that provided full gravitational support of the right arm and were fitted with an adjustable arm brace and chest restrained to minimize movements of the trunk, wrist and scapula. A cursor representing finger position was projected into the mirror placed above the arm. Direction vision of the subjects' arm was blocked and the cursor representing their index finger is provided to guide the reaching movement (Fig. 3.1.A). The KINARM was integrated with a virtual reality system that projected visual

targets on the display to make them appear in the same plane as the arm. Direct vision of the subject's arm was blocked; and a cursor representing their index fingertip was provided to guide reaching movement. The two-dimensional position and orientation of right limb segment was sampled at 1,000Hz, low-pass filtered at 15Hz, and differentiated to yield resultant velocity and acceleration values. Movement onset and offset were defined by the last minimum (below 5% maximum tangential velocity) prior to and the first minimum (below 5% maximum tangential hand velocity) following the maximum in the tangential hand velocity profile, respectively. Computer algorithms for data processing and analysis were written in MATLAB.

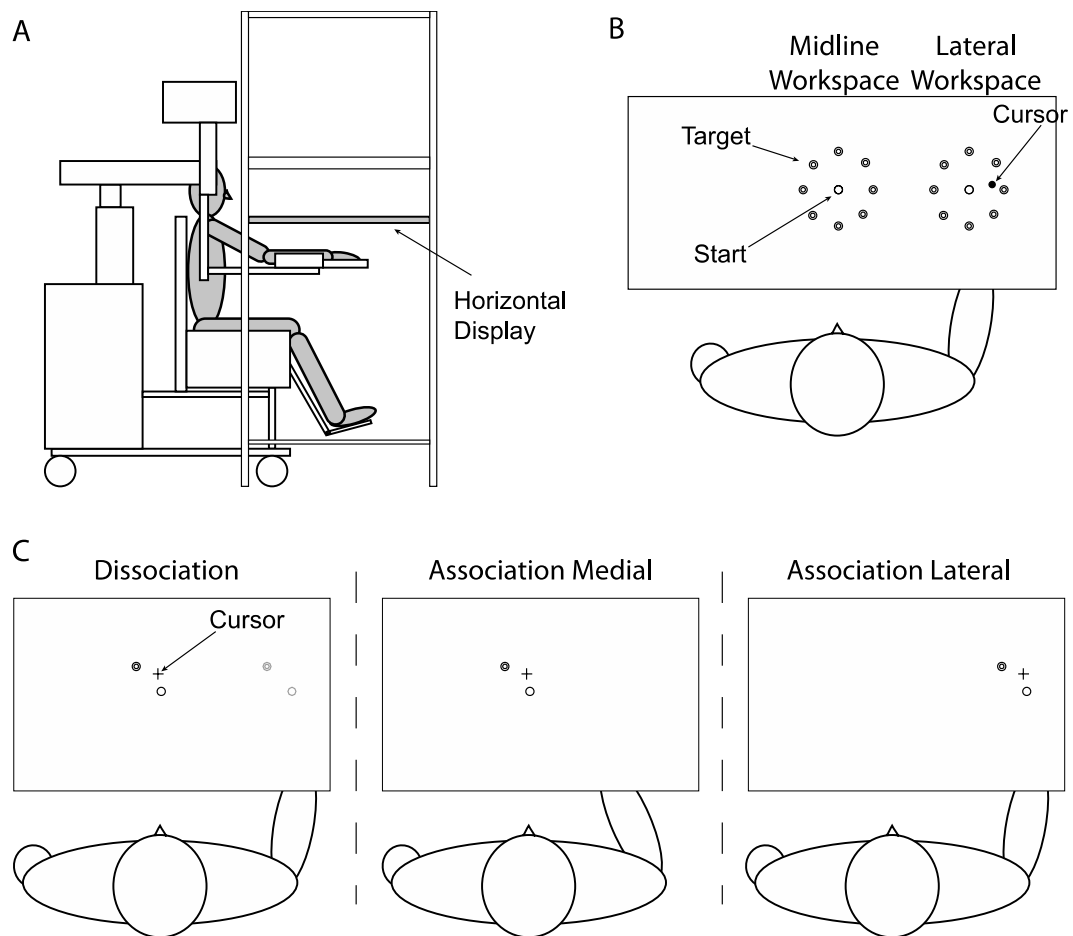


Figure 3.1, Experimental setup. A, side view: subject was seated on the chair with the right arm supported by the horizontal display. B: target was randomly displayed on one of the eight target positions. C: three sensorimotor learning conditions.

### 3.3.3 Experimental sessions

Subjects performed rapid reaching movements with the dominant arm, made from a start circle to one of eight targets (3 cm in diameter, 10 cm away from the start position) presented in a pseudo-random sequence with each cycle (i.e., 8 consecutive trials that included all 8 target directions) on the horizontal tabletop (Fig. 3.1.B). The subjects were instructed to move their index finger from the starting circle to the target as straight and fast as possible. The experiment consisted of three sessions: baseline (no rotation, 96 trials), training (30 degree rotation of visual display, 192 trials) and generalization sessions (30 degree rotation of visual display, 192 trials). In the baseline session, subjects were familiarized with the general reaching task made in the eight target directions. In the training and the generalization sessions, the subjects adapted to a visual display that was rotated 30 degrees counterclockwise (CCW) about the start circle (e.g., hand movement made in the “12 clock” direction resulted in cursor movement made in the “11 clock” direction).

During the training and generalization sessions, the subjects performed the adaptation task in one of the three experimental conditions: dissociation, association medial, and association lateral. In the dissociation (Dissoc) condition, visual and motor workspaces were separated in such a way that the cursor and the targets were presented in midline, while the subjects physically performed the adaptation task laterally (Fig. 3.1.C, left). The distance between the two start circles was 40cm. In the association medial

(AssocM) condition, the cursor and the targets were presented in midline, and the subjects performed the task in the same midline workspace (Fig. 1C, middle). In the association lateral (AssocL) condition, the cursor and the targets were presented laterally, and the subjects performed the task laterally (Fig. 3.1.C, right).

Table 3.1: Subject groups

Group (n = 5 per group)	Session	
	Training (30 deg rotation, 192 trials)	Generalization (30 deg rotation, 192 trials)
1. Dissoc-to-AssocM	Dissociation	Association Medial
2. Dissoc-to-AssocL	Dissociation	Association Lateral
3. AssocM-to-AssocL	Association Medial	Association Lateral
4. AssocL-to-AssocM	Association Lateral	Association Medial
5. Dissoc-to-Dissoc	Dissociation	Dissociation
6. AssocM-to-AssocM	Association Medial	Association Medial
7. AssocL-to-AssocL	Association Lateral	Association Lateral

To examine generalization of visuomotor adaptation from one workspace to another, subjects were divided into four experimental and three control groups (Table 3.1). Those in the first two groups (groups 1 and 2) adapted to the rotated display under the dissociation condition in the training session. Following that, they performed the same adaptation task under one of the two association conditions in the generalization

session (AssocM and AssocL). Those in the next two groups (group 3 and 4) adapted to the rotated display under one of the two association conditions in the training session; then performed the adaptation task under the other association condition in the generalization session. Additional subjects were tested in the control groups: they experienced the same experimental condition in both the training and the generalization sessions (group 5, 6, and 7).

### **3.4 Data analysis**

Two measures of performance were calculated: hand-path direction error at peak tangential arm velocity ( $V_{\max}$ ) and final position error. Initial direction error at  $V_{\max}$  was calculated as the angular difference between the vectors defined by the target and by the hand-path position at movement start and at peak arm velocity ( $V_{\max}$ ). Final position error was calculated as the 2-D distance between the index finger at movement termination and the center of the target.

For statistical analysis, data from the training and generalization sessions were subjected to two separate repeated-measures ANOVAs to examine the change of performance with time in training and generation sessions in each group: one to assess whether performance in one condition improved over time (i.e., whether learning occurred), and the other to test whether performance in another condition changed over time (i.e., whether the training in one condition generalized to another condition). Two ANOVAs were conducted with group as between-subject factor, and cycle (i.e., mean of eight consecutive trials) as a within-subject factor. Following that, post hoc comparisons, using paired t-tests, were conducted between cycle 1 of generalization session and the

mean of last 6 cycles of training session to determine whether there was a significant transfer (in experimental subject groups), or retention of learning (in control subject groups), from the training session to the generalization session within each group. In addition, to compare the course of learning between two subject groups (Dissoc-to-AssocM, Dissoc-to-AssocL) during the generalization session, a line of approximation was constructed for each subject in every subject group by finding a nonlinear logarithmic regression line. The slope, which represented generalization rate throughout the course of generalization session, and the intercept of the regression equations obtained from each subject, which represented the amplitude of error in the beginning of generalization, were subjected to independent t-tests. The alpha level was set at 0.05 for all statistical significance.

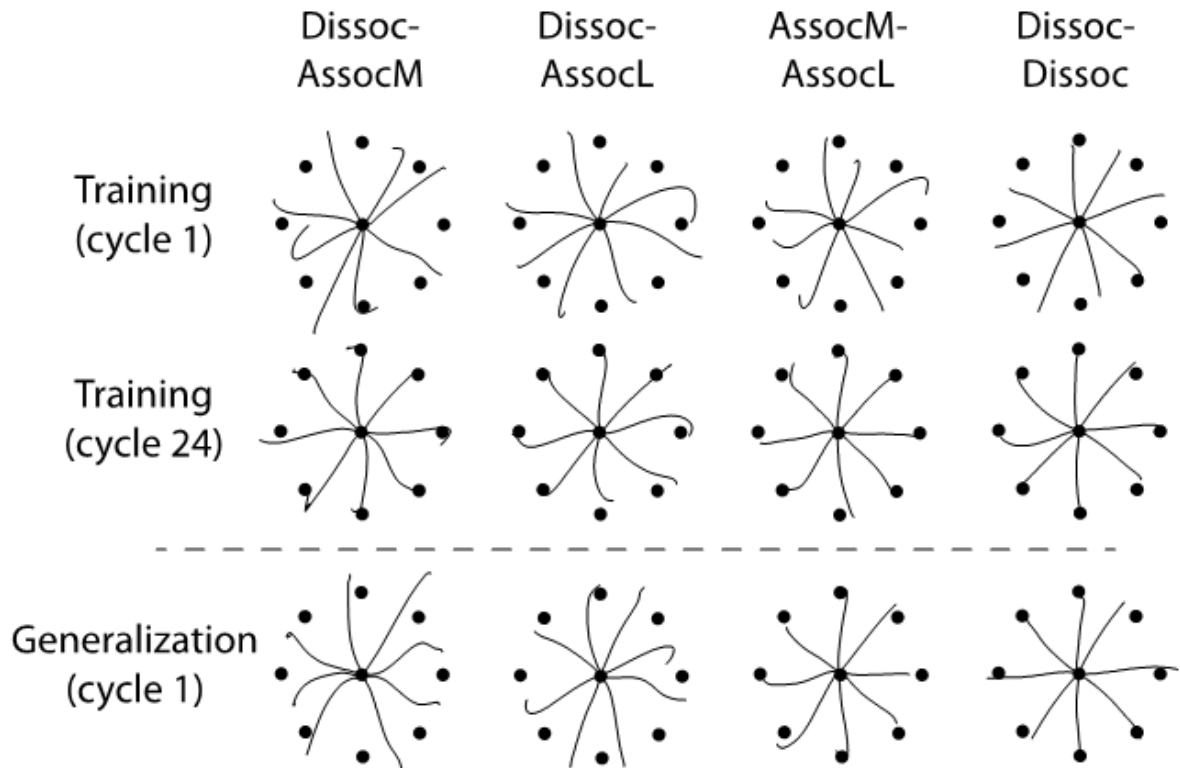


Figure 3.2, Hand-paths from representative subjects. Each column shows hand-paths of the eight consecutive trials of reaching movement made in eight different targets directions in Dissoc- AssocM (column 1), Dissoc- AssocL (column 2), AssocM- AssocL (column 3) and Dissoc- Dissoc (column 4) groups, respectively. Row 1: the first 8 trials during the training session; Row 2: the last 8 trials during the training session; Row 3: the first 8 trials during the generalization session. Black circles indicate the final target positions.

## 3.5 Results

### 3.5.1 Hand-path

Figure 3.2 shows typical hand-paths of our representative subjects during the initial and final phase of the training session, and during the initial phase of the generalization session. These hand-paths are only shown for four subject groups: three

experimental groups (groups 1~3) and one control group (group 5): the hand-paths were very similar between 3 and 4, and among groups 5~7.

The hand-paths obtained during naïve performance upon initial exposure to the visual rotation are deviated approximately  $20^{\circ}$ - $30^{\circ}$  degrees CCW from a straight line to the target (Fig. 3.2, row 1), indicating the influence of the visuomotor rotation. Following adaptation to visual rotation, hand-paths in all performance groups become fairly straight and substantially more accurate (Fig. 3.2, row 2), indicating substantial visuomotor adaptation. During generalization session, however, the arm performance appears to substantially differ across the groups (row 3): The hand-paths observed at the first cycle of the generalization session were largely curved and inaccurate in the Dissoc-to-AssocM and the Dissoc-to-AssocL groups, indicating limited transfer of visuomotor adaptation from the training to the generalization session. In contrast, the hand-paths of all the other groups (including the groups not shown in fig. 3.2) were relatively straight and accurate, indicating substantial transfer.

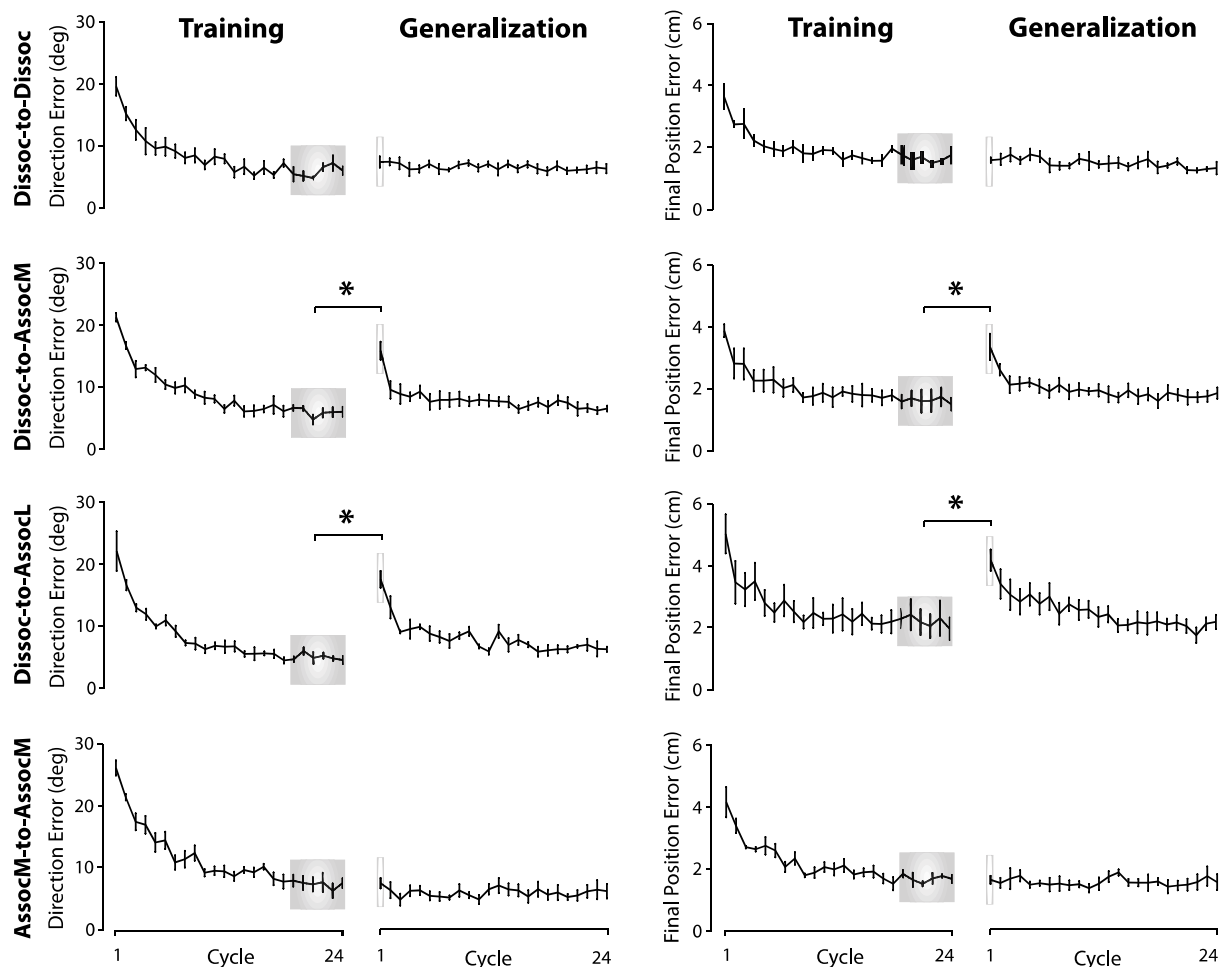


Figure 3.3, Mean performance measures of direction error (DE) and final position error (FPE).

Every data point shown on X axis of line graphs represents the mean ( $\pm$  SE) of 8 consecutive trials (cycle) across all subjects. \* indicates that comparisons between mean of cycle 1, or last 6 cycles, from training session and mean of cycle 1 from generalization session are significantly different ( $P < .05$ ). Top and bottom of vertical bars indicate mean DE and FPE at cycle 1 and cycles 19~24 from training session; horizontal line inside the bars indicate DE and FPE ( $\pm$  SE) at cycle 1 from generalization session, reflecting extent of transfer (%).

### 3.5.2 Directional and positional information

As stated above, a visual observation of hand-paths indicated the negative effect of visual and motor workspace dissociation on the generalization of visuomotor adaptation. In order to confirm this, we calculated direction error at peak velocity and final position error, which were subjected to statistical analyses. These data indicated that the extent of generalization was smaller in the subject groups who were trained in the dissociation condition and tested in the association conditions, which was confirmed by our performance measures in figure 3.3.

The repeated-measures ANOVA indicated a significant main effect for cycle ( $P < .05$ ), but not for group, in the training session. No interaction effect was observed, either. In the generalization session, however, a significant interaction effect between group and cycle was observed ( $P < .05$ ), mainly due to the fact that the patterns of adaptation across the cycles observed in the Dissoc-to-AssocM and the Dissoc-to-AssocL groups were very different from those observed in all the other groups. The paired t-tests between the first cycles of the training and generalization sessions indicated a significant difference in every group except the Dissoc-to-AssocL group, in which the lack of significance was due to larger variability caused by one subject. Those between the mean of the last six cycles of the training session and the first cycle of the generalization session indicated a significant difference in the Dissoc-to-AssocM and the Dissoc-to-AssocL groups ( $P < .01$ ), while the two values were not significantly different in all the other groups. The one-way ANOVA using the percentage scores also indicated a

significant difference across the subject groups ( $P < .01$ ). The post hoc tests revealed that the two dissociation groups, which were not different from each other, were significantly different from the association groups, which were not different from each other.

### **3.5.3 The rate of generalization**

With regard to the course of learning in the Dissoc-to-AssocM and the Dissoc-to-AssocL groups during the generalization session, the rate of adaptation (in terms of both direction and final position errors) appeared somewhat faster in Dissoc-to-AssocM condition than in the other condition. We then conducted a further analysis by finding a nonlinear logarithmic regression line for direction and final position performance in generalization sessions of Dissoc-to-AssocM and Dissoc-to-AssocL group. The slope, which represented the rate of generalization, and the intercept, which represented the amplitude of errors at the beginning of generalization, of the regression equation obtained from each subject for each group were subjected to independent t-tests. The independent t-tests showed that neither the intercept nor the slope of the regression equations was significantly different between the two subject groups, which indicated that the pattern, or the rate, of adaptation during the generalization session was similar between the two groups. The regression equations for the Dissoc-to-AssocM group were  $Y = 12.37 - 1.91 \ln(X)$  and  $Y = 0.027 - 0.004 \ln(X)$  in terms of direction and final position errors, respectively; and those for the Dissoc-to-AssocL group were  $Y = 14.69 - 2.81 \ln(X)$  and  $Y = 0.038 - 0.006 \ln(X)$  Data in terms of direction and final position errors, respectively, as shown in Figure 3.4.

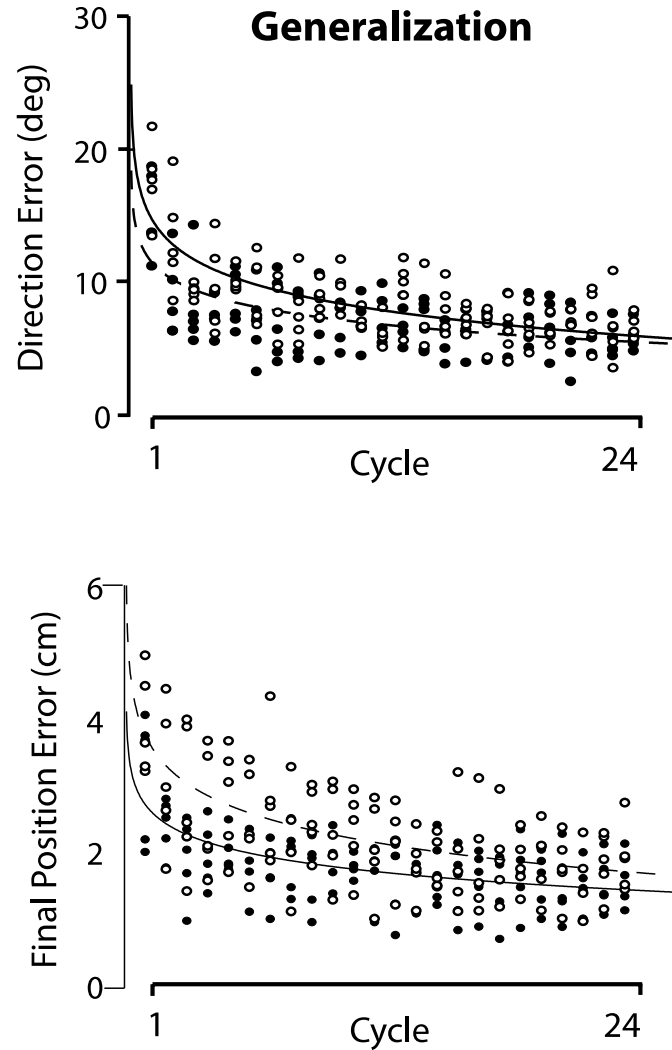


Figure 3.4, Mean performance measures of direction error at peak tangential arm velocity (top) and final position error (bottom) are shown for Dissoc-to-AssocM group (filled circles) and Dissoc-to-AssocL group (open circles) during generalization session. Every data point shown on the x-axis represents the average of consecutive trials across all subjects. Solid black lines represent nonlinear logarithmic curve fits for the performances of generalization sessions in Dissoc-to-AssocM group, while broken lines represent those for the performances of generalization sessions in Dissoc-to-AssocL group.

### 3.6 Discussion

In this study, we examined the effect of separating visual and motor workspaces during targeted-reaching movement on generalization of visuomotor adaptation across different workspace conditions in which the same arm was used. When the subjects first adapted to a 30-degree visual rotation under a condition in which the visual and motor workspaces were combined with each other, complete generalization was observed from one workspace to another (from medial to lateral workspace, or vice versa). This finding is consistent with previous findings, which demonstrate generalization of visuomotor adaptation across different workspaces (Heuer et al. 2011, Krakauer et al. 2000, Vetter et al. 1999, Wang et al. 2005). In our current study, however, when the subjects first adapted to a visuomotor rotation under a condition in which the visual and motor workspaces were separated, the extent of generalization was much smaller than that observed in the other condition in which the two workspaces were combined. This finding indicates that the separation of visual and motor workspaces has a substantial influence on the pattern of generalization.

We have previously demonstrated that the pattern of interlimb transfer depends on the workspace locations in which the two arms perform visuomotor tasks. We observed asymmetrical transfer of movement information (e.g., directional information transferring from nondominant to dominant arm, not vice versa) when both arms adapted to a visual rotation in a shared midline workspace (Sainburg et al. 2002), but symmetrical transfer (e.g., directional information transferring in both directions) when each arm adapted in its ipsilateral workspace (Wang et al. 2006). This suggests that when visuomotor tasks are performed in workspaces that are not shared by the arms, both arm controllers have

symmetrical access to the information acquired by the opposite arm controller. When the tasks are performed within a shared workspace, however, a certain competition may occur between the arm controllers, which selectively inhibit each controller from accessing the information for which the other controller is specialized, thus resulting in asymmetrical transfer. Other studies suggested that the dominant and nondominant limb/hemisphere systems are differentially specialized for controlling directional and positional features of movement, respectively (Bagesteiro et al. 2002, 2003). This idea of selective inhibitions between the arm controllers was inspired by the findings reported by Gazzaniga and colleagues (Franz et al. 1996; Holtzman et al. 1982), which indicated that cognitive and motor processes that take place in each brain hemisphere can interfere with each other when the processes involve processing two incompatible sets of information.

The pattern of interlimb transfer is influenced even more when visual and motor workspaces are separated: interlimb transfer does not occur at all when each arm performs visuomotor tasks in its ipsilateral workspace while the visual display is presented in midline, or vice versa (Wang et al. 2008). The lack of interlimb transfer in that situation may indicate that a conflict between visual and motor workspaces inhibits each arm controller from accessing the movement information obtained by its counterpart, because of uncertainties in determining hand dominance at a given workspace. Alternatively, such a conflict may lead to incomplete development of a neural representation associated with a given visuomotor condition. If the former explanation is correct, a conflict between visual and motor workspaces should not interfere with generalization of visuomotor adaptation across movement conditions in which the same arm is used. However, if the latter explanation is correct, the conflict should also disturb

within-arm generalizations. The current study demonstrated limited transfer across movement conditions within the same arm under the conditions in which visual and motor workspaces were separated, which supports the latter view that a conflict between visual and proprioceptive information in terms of workspace locations disrupts the development of a neural representation associated with a novel visuomotor condition.

When one adapts to a novel sensorimotor condition, two types of internal models may be developed, one based on visual information and the other based on proprioceptive information, which combine to guide reaching performance (Hwang et al. 2006). This is in agreement with the idea that the planning of reaches to visual and proprioceptive targets may involve distinct sensorimotor transformations (Bernier et al. 2007). Based on these ideas, we speculate that separating visual and motor workspaces caused the relationship between the two types of sensory information and the two types of internal models to depend on the nature of a given workspace. That is, when subjects viewed their performance in a midline workspace while physically performing the adaptation task in a lateral workspace, an internal model was formed in relation to the midline workspace, which primarily relied on the visual information regarding the subjects' performance, and another model in relation to the motor workspace, which primarily relied on their proprioceptive information. In this condition, combining the two internal models would create a serious computational problem because the visual and proprioceptive estimates of limb state represented in one model would not match with those represented in the other model. This would disrupt the development of an overall neural representation that underlies adaptation to a novel visuomotor transform, which in turn would negatively

affect generalization of that adaptation not only across the limbs, but also across different workspace conditions within the same limb.

In this study, we also compared the course of adaptation between two subject groups in which visuomotor adaptation acquired under the dissociation condition was generalized to an association condition in which either the visual or the motor workspace was the same as that in the dissociation condition (AssocM and AssocL, respectively). Our results indicated no difference between the two subjects groups in terms of the intercept or the slope of regression equations. This suggests that the vision-based and the proprioception-based models contribute equally to the development of the overall representation underlying visuomotor adaptation. Considering that visual and proprioceptive information may play differential roles in the planning and execution of reaching movement (Sainburg et al. 2003; Sober et al. 2003), however, additional research is needed to better understand the roles of these two internal models in sensorimotor adaptation and its generalization across movement conditions.

### **3.7 Study limitations**

The lack of difference observed between the two dissociation groups (Dissoc-AssocM, Dissoc-AssocL) may be attributed to the fact that we only had five subjects in each group. The reason why we selected a small sample size is that the study demonstrated statistically significant differences for our major concerns using such a small sample. It is possible that the selected sample may not be a good representative of its population. However, such possibility always exists even with quite a large sample size. Including additional subjects in these groups might affect the results and possibly demonstrate that the rate of generalization could significantly differ between the two

conditions, because when the study fails to observe statistically significant differences, sample size pose a serious concern.

### **3.8 Conclusion**

Dissociation of visual and motor workspaces during targeted reaching movement has been shown to disrupt transfer of visuomotor adaptation across the arms. This suggests that a conflict between visual and proprioceptive information in terms of workspace locations may disrupt the development of neural representations underlying visuomotor adaptation. In this study, we tested the effects of visual and motor workspace dissociation on the generalization of visuomotor adaptation across different conditions within the same arm. Subjects were divided into seven groups: those in the first three groups adapted to a rotated visual display under a “dissociation” condition in which the visual workspace was presented in midline while the task was physically performed laterally from midline. During the subsequent generalization session, one of the three groups performed the same adaptation task in the dissociation condition again, and the other two groups under an “association” condition in which the visual and motor workspaces were overlapped either in midline (association medial) or at a lateral workspace (association lateral). Subjects in the other four groups adapted to the rotation in either the association medial or lateral condition during the adaptation session, and in either of the two conditions again during the generalization session. Nearly complete generalization occurred from the training to the generalization session in the first group (dissociation to dissociation) and the last four groups (association to association), whereas the extent of generalization was substantially smaller in the other two groups (dissociation to association). These findings suggest that a conflict between visual and

proprioceptive information in terms of workspace locations may disrupt the development of a neural representation, or an internal model, that is associated with visuomotor adaptation, which results in limited generalization of visuomotor adaptation.

## Chapter 4

### **Brain activation associated with the generalization of visuomotor adaptation: an fMRI case study**

#### **4.1 Introduction**

Individuals have an ability to adapt their movements in response to both visual and mechanical perturbations. One of the common paradigms that have been widely used to study this ability involves visuomotor adaptation tasks, in which a perturbation that distorts the visual consequence of the motor commands is introduced (Welch et al, 1974; Bock, 1992; Ghilardi et al, 2000). Numerous neuroimaging studies that employed visuomotor adaptation tasks have suggested that a visuomotor adaptation process recruits a variety of cortical and subcortical brain regions in a time-dependent manner, these include the primary motor cortex (M1), prefrontal cortex (PFC), parietal cortex, supplementary motor area (SMA), cerebellum, and striatum in the early adaptation (Ghilardi et al. 2000; Imamizu et al. 2000; Inoue et al., 2000; Miall et al. 2001; Krakauer et al. 2004; Graydon et al. 2005; Seidler et al. 2006). During the late stages of adaptation, activation has been observed in the cerebellum, as well as the visual, parietal and temporal cortices (Imamizu et al. 2000; Inoue et al. 2000; Miall et al. 2001; Krakauer et al. 2004; Graydon et al. 2005). In particular, the cerebellum is thought to play a crucial role in adaptation. Taylor and Ivry (2010) found that during adaptation to a visuomotor task, cerebellar patients were able to implement the cognitive strategy to predict movement errors without interfering with the adaptation, which was consistent with the finding that implicit adaptation to a visuomotor task overrides explicit cognitive strategy in visuomotor adaptation (Mazzoni and Krakauer 2006). A brain stimulation study (Galea

et al. 2010) further confirmed the cerebellum's involvement in sensorimotor adaptation. In this study, the investigators reasoned that enhancing cerebellar activity should be able to facilitate the rate of adaptation if the cerebellum adjusts forward models in incremental steps on a trial-by-trial basis, which is what they found.

As discussed in chapter 1, an internal model represents a memory of prior learning, which could be used for subsequent learning. The cerebellum is thought to play a role in storing an internal model of the motor apparatus (Ramnani 2006; Ito 2008). Shadmehr and Holcomb (1997) conducted a task in which subjects were asked to learn to move an object with complex dynamics, and then performed the task again after a 6-hour delay. Increased activations were in the right anterior cerebellar cortex from the late learning to the recall phase, which suggests that after initial learning, an internal model is stored in the cerebellum. These studies suggested that the reduction of errors during adaptation is a cerebellum-relevant process. In contrast, the primary motor cortex (M1) is identified to be involved in the retention of the learnt visuomotor transformation (Richardson et al. 2006; Hadipour-Niktarash et al. 2007; Hunter et al. 2009). For example, Richardson et al. (2006) identified the primary motor cortex (M1) as a key region in motor learning with repetitive transcranial magnetic stimulation (rTMS), and found M1 was important for initiating the development of long-term motor memories.

Evidence that the parietal region plays a role in visuomotor adaptation comes, in part, from prism adaptation. Clower et al (1996) examined brain activation, utilizing positron emission tomography, in participants who performed pointing movement while wore lateral displacement prisms. Consistent activations were observed in the posterior parietal cortex contralateral to the pointing arm. Another study from Fernandez-Ruiz et al.

(2007) provided further support for PPC participation in visuomotor adaptation. In this study, they had participants perform pointing movement wearing left/right reversing prisms, and found that the PPC region responded more for planning ipsilateral pointing movement than contralateral to movement direction. This finding suggests that the PPC does not primarily encode in strictly vision and movement coordinates but rather plays an important role as an intermediary between visual and motor coordinates. Like PPC, the frontal cortex also has been identified as playing some roles in visuomotor adaptation. The neurophysiological evidence shows that the frontal cortex is involved in motor planning and preparation. For example, Praeg and colleagues (2005) proposed that PMC is not correlated with sensorimotor learning, but rather involved in movement preparation.

Smith et al. (2006) suggested that short-term motor adaptation involves two distinct adaptive processes: one process induces fast learning but has poor retention, whereas the other leads to slow learning but retains information very well. Based on this idea, Seidler et al. (2008) reasoned that the brain regions that were more active during the fast, initial stage of adaptation would not be involved in transfer of motor learning, because the learning process involved in this early stage of learning would decay quickly. In that study, they found that brain regions involved in the early stage of adaptation showed reduced activity at transfer, which included the right inferior frontal gyrus, primary motor cortex, inferior temporal gyrus, and the cerebellum. These studies have helped us to identify the brain regions that are involved in visuomotor adaptation, although further research is necessary to better understand the neural mechanisms underlying the generalization of visuomotor adaptation across different movement conditions.

## 4.2 Purpose

The purpose of this study was to use fMRI to investigate the neural activity involved in the generalization of visuomotor adaptation across movement conditions in which the visual and motor workspaces during reaching movement were either dissociated or associated with each other. We developed a visuomotor rotation task using the MovAlyzeR, 2D movement data acquisition software, which required subjects to use an MR-compatible joystick to perform reaching movements with their right arm. This enabled us to examine brain activity during three movement conditions that were similar to those employed in our behavioral study (chapter 3). Two of the three conditions, Dissoc-to-AssocL and Dissoc-to-AssocR, were analogous to the Dissoc-to-AssocM and the Dissoc-to-AssocL conditions in our behavioral study; and the last condition, AssocL-to-AssocL was analogous to the AssocL-to-AssocL condition (control condition).

Based on the findings from our behavioral study that initial adaptation under the two dissociation conditions resulted in limited generalization to the association conditions, it was hypothesized (1) that the cerebellum would only be active during the generalization session in the AssocL-to-AssocL condition, and not in the other two conditions. The rationale for this hypothesis was that the internal model developed under the association condition in the training session, which was stored in the cerebellum, would be readily available to facilitate the reaching movements under the same condition in the generalization session. The internal model developed under the dissociation condition in the training session, however, would not be very useful for performing the task under the association condition in the generalization session. It was also hypothesized (2) that the brain activity observed at the initial stage of the training session

would be similar to that observed at the initial stage of the generalization session in the Dissoc-to-AssocL and Dissoc-to-AssocR conditions, and (3) that the brain activity observed at the final stage of the training session would be similar to that observed at the initial stage of the generalization session in the AssocL-to-AssocL condition. The rationale for the second hypothesis was that because the internal model developed under the dissociation condition in the training session would not be very useful for performing the reaching task under the association condition in the generalization session, it would require a new internal model to be developed in the generalization session (thus similar brain activity observed at the initial stage of both sessions). In contrast, because the internal model developed in the training session would also be used in the training session in the AssocL-to-AssocL condition, the brain activity would be similar between the final and the initial stage of the training and the generalization session, respectively (the third hypothesis).

### **4.3 Methods**

#### **4.3.1 Subject**

Three neurologically intact subjects (two males and one female) between 20 and 26 years old participated in the experiment (one subject per condition), after giving a written informed consent according to the Declaration of Helsinki and institutional guidelines at Marquette University, University of Wisconsin, Milwaukee and the Medical College of Wisconsin. All subjects were right-handed (handedness of the subjects were determined using the 10-item version of Edinburgh Handedness Inventory). All subjects had an MR safety interview and were excluded if they were claustrophobic, pregnant, or

had any implants or foreign bodies incompatible with fMRI. Subjects were also excluded if they had a history of neurological impairments. Subjects were paid for their participation. The subjects completed a familiarization training session before they went to the scanning room. During fMRI scanning, subjects lay supine on the scanner bed in a 3.0-T magnet (General Electric), with their head inside 32- channel head coil. In order to minimize head movement, a beaded vacuum pillow was placed underneath the head. A head strip across the forehead was used to keep the head stable; and two additional straps across the abdomen and the legs were used to minimize the body movement. Subjects were required to only move their hand during the scanning. Subjects were able to view the screen on top of their eyes, in which tasks and instructions were projected via the reflected mirror. Subjects had a set of headphones on top of their ears to protect against the scanner noise, and held an emergency squeeze ball to signal a problem to the scanner technician.

#### **4.3.2 Experimental Task**

During the task, the MR-compatible joystick was placed on the subjects' stomach. The position of the joystick was adjusted until subjects were able to control the joystick comfortably. Subjects were instructed to hold the joystick to make rapid wrist movements with the dominant arm, made from a start circle to one of two targets (2 cm in diameter, 10 cm away from the start circle) presented on the screen in a pseudo-random sequence; no arm movements were made; Subjects viewed a rear-projected screen, which projected the visuomotor adaptation task and provided real-time feedback of movement. The joystick was used to control a cursor on the screen. Subjects first viewed a pre-cue target circle that lasted for 2 or 4 seconds, and were asked to move the cursor into the pre-cue

target circle and to maintain the cursor within the pre-cue circle until the target circle appeared. Then subjects were instructed to move the cursor to the target circle as fast and straight as possible and stop on it until the target disappeared. Upon target disappearance, the next trial began. Figure 4.1 demonstrates fMRI experimental design. The trials were presented within three sessions of activity: baseline (40 trials), training (80 trials) and generalization (40 trials). We visually monitored subjects' performance via the control room window throughout the experiment. If the subjects did not perform the task as instructed or their head movement was more than 2 mm, then we would repeat the instruction, asked subject to adjust their movement.

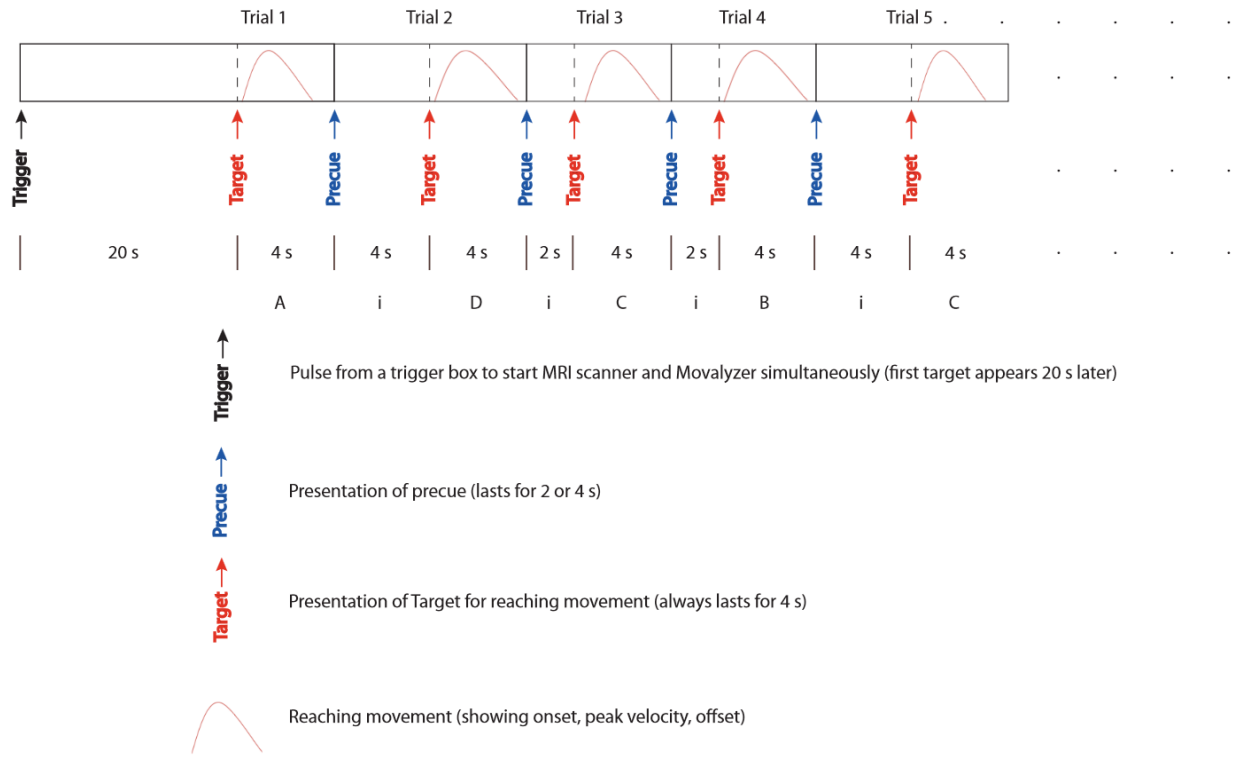


Figure 4.1, Experimental design: Subjects first view a pre-cue target circle that lasts for 2 or 4 seconds, and are asked to move the cursor into the pre-cue target circle and to maintain the cursor within the pre-cue circle until the target circle appears. Then subjects are instructed to move the

cursor to the target circle and stop on it until the target disappears that always lasts for 4s. Upon target disappearance, the next trial begins.

### **4.3.3 Experimental sessions**

The subjects completed a familiarization training session in mock room before they went to the scanning room. During fMRI scanning, the experiment consisted of three sessions: baseline (no rotation, 40 trials), training (30 degree rotation of visual display, 80 trials) and generalization sessions (30 degree rotation of visual display, 40 trials). Subjects were first familiarized with the general reaching task made in the two target directions during the baseline session, then adapted to a novel visual rotation. The position of the cursor was rotated 30 degrees counterclockwise (CCW) about the start circle (e.g., hand movement made in the “12 clock” direction resulted in cursor movement made in “11 clock” direction) during the training and generalization sessions.

Table 4.1: Experimental design

Condition (n = 1 per condition)	Session	
	Training (30 deg rotation, 80 trials)	Generalization (30 deg rotation, 40 trials)
1. Dissoc-to-AssocL	Dissociation	Association Left
2. Dissoc-to-AssocR	Dissociation	Association Right
3. AssocL-to-AssocL	Association Left	Association Left

During the training session, the subjects were tested in three conditions (one subject per condition; see Table 4.1). The subjects in the first two conditions, Dissoc-to-AssocL and Dissoc-to-AssocR, adapted to the visual rotation under a condition in which visual and motor workspaces were dissociated with each other (fig. 4.2. mid panel). The subject in the last condition, AssocL-to-AssocL, performed the same task under a condition in which visual and motor workspaces, located on the left side from the body midline, were associated with each other (fig. 4.2, left panel). During the subsequent generalization session, all subjects performed the same task under the condition in which the two workspaces were associated with each other. The subjects in the first and the last conditions experienced the associated workspaces presented on the left side, and the subject in the second condition on the right side of the midline (fig. 4.2, right panel).

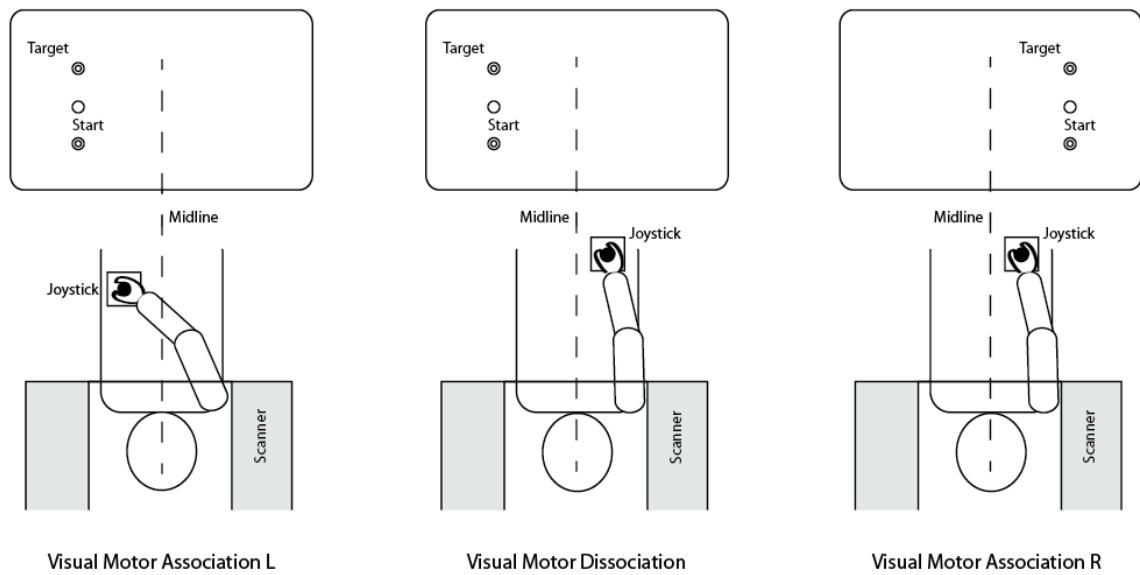


Figure.4.2, Left, Schematic diagram of VMAL; Mid, Schematic diagram of VMD; Right, Schematic diagram of VMAR;

#### 4.3.4 Behavioral data processing

The data acquisition software called MovAlzyeR was used to record the X and Y coordinates from the joystick at a rate of 200Hz. The data were filtered with a low pass Butterworth digital filter using a cutoff frequency of 10Hz. The cursor-path was calculated by computing the square root of the sum of the squared X and Y coordinate data at each time point. The velocity and acceleration profiles were calculated through differentiation. Movement onset and offset were defined by the last minimum (below 5% maximum tangential velocity) prior to and the first minimum (below 5% maximum tangential hand velocity) following the maximum in the tangential hand velocity profile, respectively. Computer algorithms for data processing and analysis were written in MATLAB.

Two measures of performance were calculated: hand-path direction error at peak tangential arm velocity ( $V_{\max}$ ) and final position error. Initial direction error at  $V_{\max}$  was calculated as the angular difference between the vectors defined by the target and by the hand-path position at movement start and at peak arm velocity ( $V_{\max}$ ). Final position error was calculated as the 2-D distance between the index finger at movement termination and the center of the target.

#### **4.3.5 fMRI acquisition parameters**

fMRI images were obtained using a gradient echo, echo planar imaging (EPI) pulse sequence with 44 contiguous slices in the sagittal plane, 3.5 mm slice thickness, echo time (TE) = 25 ms, interscan period (TR) = 2 s, flip angle = 77°, field of view (FOV) = 24 cm, and 64 x 64 matrix). The resolution of the images was 3.5 x 3.5 x 3.5 mm. Anatomical images (SPGR) were acquired using TE = 3.9 ms, TR = 9.5 ms, flip angle = 12° with a field of view of 256 x 244 mm; and slice thickness was 1mm.

#### **4.3.6 fMRI data processing**

fMRI data were processed and analyzed using the Analysis of Functional NeuroImages (AFNI) software. The first and the last 100 TRs within the training session were regarded as early and later adaptation periods, respectively; the first 100 TRs within the generalization session was taken as generalization period. A graphic user interface named 'uber\_subject.py' was used for running subject analysis. Below summarizes the steps performed in the program (see Appendix for a detailed flow chart):

The first four TRs within each session were removed to eliminate magnetization artifact so as to allow the MRI signal to reach its steady state. The base EPI image was

first selected, and then anatomical image was registered to this image. The rest of EPI images were then aligned to the base image, to the anatomic image and warped to Talairach space. The head movement in six dimensions (x, y, z-axes, pitch, yaw and roll) was reported as the result of the alignment. These images were spatially smoothed with a full width at half maximum (FWHM) Gaussian filter and normalized to a mean of 100 in each voxel time series to reduce noise and to diminish the multiple comparison problems.

The ideal hemodynamic response function was defined by using the ‘‘TENT’’ function. The hemodynamic response function (HRF) is expressed by the linear combination of a finite set of basic functions  $\omega_q(t)$ , such as equation 4.1.

$$h(t) = \beta_0 \omega_n(t) + \beta_1 \omega_1(t) + \beta_2 \omega_2(t) + \dots = \sum_{q=0}^{q=p} \beta_q \omega_q(t) \quad \text{Eq. 4.1}$$

where  $\beta$  is the weight and  $p$  is the expansion order. A larger  $p$  represents more complex shapes and more parameters.

Regarding the HRF at any arbitrary point in time after the stimulus times, the equation 4.2 allows for calculation of sum of HRF copies.

$$\gamma_n = \sum_{k=1}^K h(t_n - \tau_k) \quad \text{Eq. 4.2}$$

In our case, the basic function is the tent function, which can be described using equation 4.3.

$$T(x) = \begin{cases} 1 - |x| & \text{for } -1 < x < 1 \\ 0 & \text{for } |x| \geq 1 \end{cases} \quad \text{Eq. 4.3}$$

Expansion of HRF in a set of spaced-apart tent functions is the same as linear interpolation between ‘‘knots’’

$$h(t) = \beta_0 T\left(\frac{t}{L}\right) + \beta_1 T\left(\frac{t-L}{L}\right) + \beta_2 T\left(\frac{t-2*L}{L}\right) + \dots \quad \text{Eq. 4.4}$$

where L is the tent function grid spacing.

TENT function has the form of “TENT (b, c, n)” in AFNI, in which b represents the stimulus onset, c represents the time span of the hemodynamic response, and n represents the number of tent functions to form HRF (AFNI website, 2009). To identify the activation, general linear modeling (GLM) was used. With GLM, the bold signal can be expressed in the following equation:

$$Y = X \beta + \epsilon \quad \text{Eq. 4.5}$$

where X is the sum of HRF copies,  $\beta$  is the least square coefficient with X, and  $\epsilon$  is the error.

“3dDeconvole” function was used to calculate the deconvolution of a measurement 3D+time dataset with a specified input stimulus time series. The output of the program consisted of a “bucket” type dataset containing the least squares estimates of the linear regression coefficients; a t-statistic describing the significance of the coefficients; a F-statistical for significance of the overall regression model.

Monte Carlo simulation was performed to set an appropriate cluster size for a given individual voxel P-value. Active regions that are not in the cluster were considered inactivate. Significantly active region outside of the brain and negatively correlated regions were also ignored.

According to the literature review, we used CA\_N27\_ML atlas to mask the following regions as our regions of interest (ROIs): primary motor cortex (M1),

prefrontal cortex (PFC), parietal cortex, supplementary motor area (SMA), temporal cortex and cerebellum. In order to quantify the activation pattern among early-adaptation, later-adaptation and generalization, we computed the activation volume. The volume of activation was calculated within ROIs using the “3dclust” function. The center of mass of each cluster and ROI were reported from the result of “3dclust”. The first 100 TRs period of the early-adaptation and early generalization, and the last 100 TRs period of the later-adaptation were processed using above steps.

## **4.4 Results**

### **4.4.1 Behavioral results**

Spatial hand-paths of three subjects are depicted in Fig 4.3 during the early and late phase of the training session, and during the early phase of the generalization session. These hand-paths are only shown for two subjects: one in the Dissoc-to-AssocL condition and one in the AssocL-to-AssocL condition. The hand-paths were very similar between the two subjects who experienced the dissociation condition in the training session.

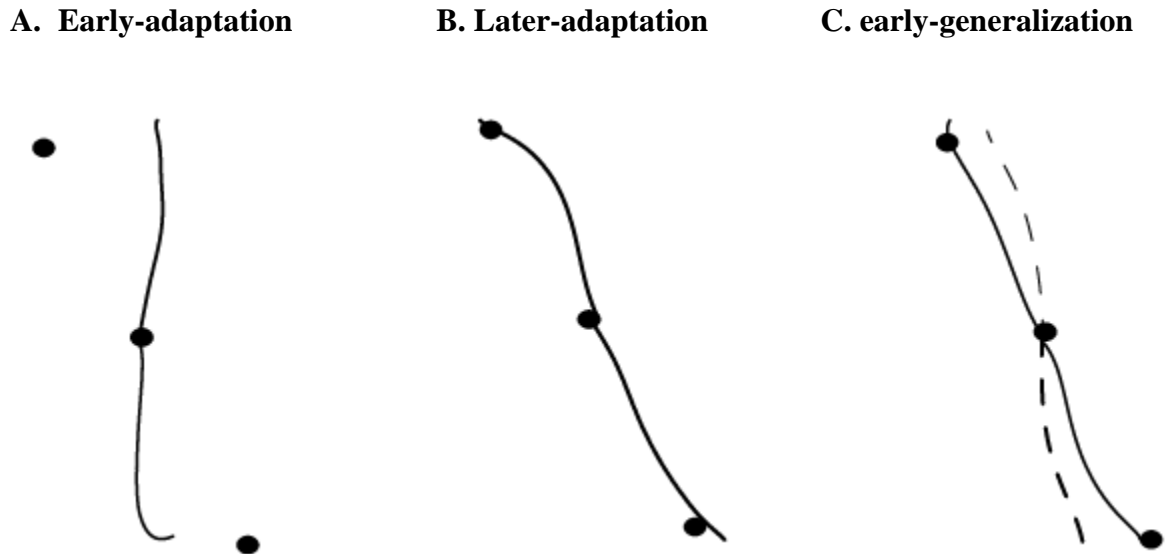


Figure.4.3, Panel A shows the hand-paths for two trials under the 30 degree feedback rotation during the early phase of the training session. Panel B depicts the hand-paths during the late phase of the training session. Panel C depicts the hand-paths from two subjects in separate condition performing 30 degree rotation during the early phase of the generalization session. Black line represents the hand-paths from the same subject in the AssocL-AssocL condition; Broken line represents the hand-paths from the subject in the Dissoc-AssocL condition. The filled circles indicate the target locations in joystick space.

The hand-paths obtained during naïve performance upon initial exposure to the visual rotation are deviated approximately  $20^{\circ}$ - $30^{\circ}$  degrees CCW from a straight line to the target (Fig. 4.3, A), indicating the influence of the visuomotor rotation. Near the end of the training session, hand-paths of all three subjects became relatively straight and more accurate (Fig. 4.3, B), indicating substantial visuomotor adaptation. During the generalization session, the performances appeared substantially different across the conditions (Fig. 4.3, C): Following initial adaptation under the dissociation condition in training session, the two subjects' performances at the beginning of the generalization session (Fig. 4.3, C, broken line) was less accurate than the performance of the subject

who initially adapted under the association condition (Fig. 4.3, C, solid line). These findings suggest that initial adaptation to the dissociation condition did not facilitate subsequent adaptation to either of the two association conditions very much (i.e., limited generalization from the dissociation to the association condition).

As stated above, a visual observation of hand-paths indicates a negative effect of the dissociation condition on generalization of visuomotor adaptation. In order to confirm this, we calculated two performance measures: direction error at peak velocity and final position error. These data indicated that the pattern of adaptation during the training session was very similar across the three subjects (Fig. 4.4). However, both direction and final position errors at the first cycle in the generalization session was much larger in the subjects who adapted under the dissociation condition in the training session than the subject who adapted under the association condition (Fig. 4.5), indicating limited generalization of visuomotor adaptation in the two dissociation conditions. These data are consistent with the data that we observed in our behavioral study (Chapter 3), in that the initial amount of transfer that occurred from the training to the generalization session was substantially smaller when the subjects adapted to the visuomotor rotation under the dissociation condition (Table 4.2) than under the association condition (Table 4.3).

---

Table 4.2 – The first 8 trials in the generalization session in the Dissoc-AssocL condition

---

Trial #	Direction Error	Final Position Error
1	21.92	0.033
2	15.90	0.028
3	14.97	0.023
4	9.76	0.020
5	9.04	0.016
6	10.66	0.022
7	10.31	0.018
8	9.43	0.018

---

---

Table 4.3 – The first 8 trials in the generalization session in the AssocL-AssocL condition

---

Trial #	Direction Error	Final Position Error
1	7.93	0.012
2	6.46	0.013
3	8.35	0.019
4	7.41	0.012
5	5.11	0.018
6	7.85	0.015
7	3.79	0.008
8	5.52	0.016

---

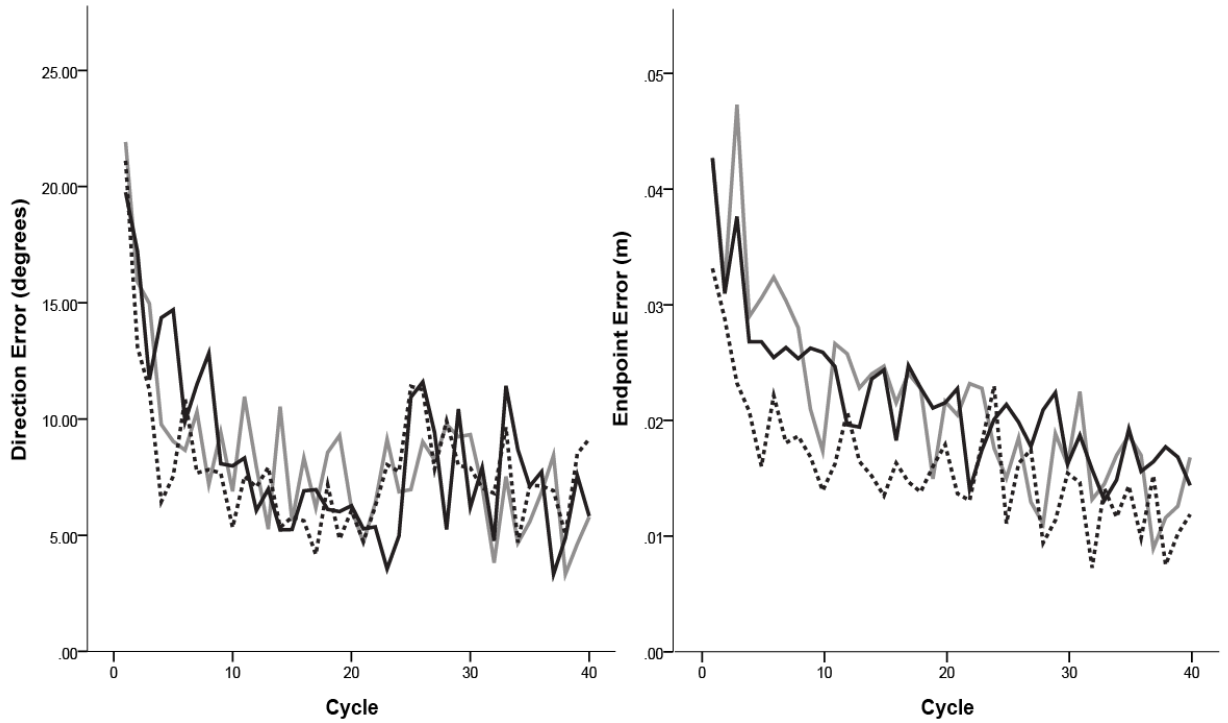


Figure 4.4, Performance measures of direction error and endpoint error during the training session. Every data point shown on X axis represents 2 consecutive trials (cycle). Performance measures for three conditions are shown. Black line represents the data from the subject in the AssocL-AssocL condition. Gray line indicates the data from the subject in the Dissoc-AssocL condition. Broken line represents the data from the subject in the Dissoc-AssocR condition.

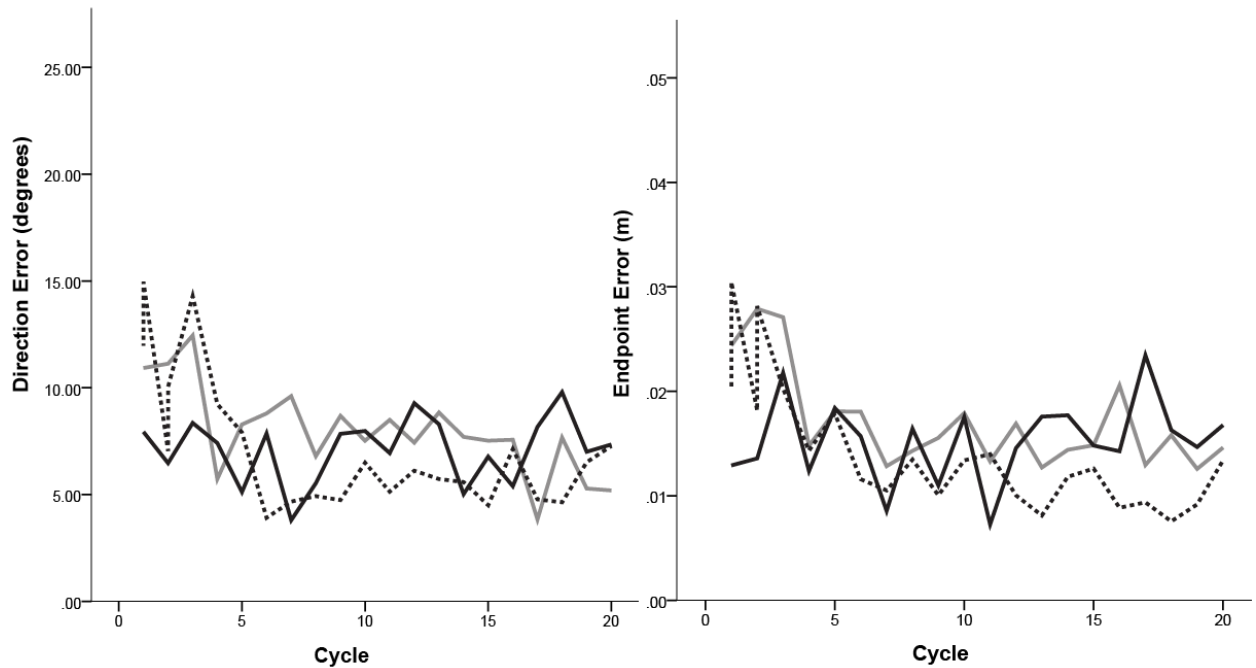


Figure 4.5, Performance measures of direction error and endpoint error during the generalization session. Every data point shown on X axis represents 2 consecutive trials (cycle). Performance measures for three conditions are shown. Black line represents the data from the subject in the AssocL-AssocL condition. Gray line indicates the data from the subject in the Dissoc-AssocL condition. Broken line represents the data from the subject in the Dissoc-AssocR condition.

#### 4.4.2 Brain activation observed during the early phase of the training session

We observed that the early training phase was primarily correlated with the brain activation in left primary motor cortex, left inferior frontal gyrus, right inferior frontal gyrus, left middle frontal gyrus, and left supplementary motor cortex (see Table 4.2, 4.3, 4.4), which were overlaid onto an anatomical slice in Figure. 4.6.

---

 Table 4.4 – Regions engaged in the Dissoc-AssocL condition
 

---

Anatomic location	Volume of Activation (mm <sup>3</sup> )		
	Early training	Late training	Generalization
L primary motor cortex	2531.1	85.8	4719
L primary sensory cortex	126.8	231	167.5
L inferior frontal gyrus	2316.6	429	557.7
R inferior frontal gyrus	2273.7	300.3	85.8
L middle frontal gyrus	1973.4	128.7	1973.4
L Supplementary motor cortex	2831.4	514.8	2616.9
R superior parietal lobule	0	2187.9	514.8
L inferior parietal lobule	514.8	4032.6	900.9
R inferior parietal lobule	171.6	1072.5	471.9
L middle occipital gyrus	300.3	3389.1	343.2
Left lobule VI (Hem)	85.8	514.8	85.8
Right lobule VI (Hem)	0	900.9	343.2

---

Table 4.5 – Regions engaged in the Dissoc-AssocR condition

Anatomic location	Volume of Activation (mm <sup>3</sup> )		
	Early training	Late training	Generalization
L primary motor cortex	1329.9	42.9	3432
L primary sensory cortex	312.1	143.2	35.2
L inferior frontal gyrus	1930.5	128.7	858
R inferior frontal gyrus	2488.2	471.9	514.8
L middle frontal gyrus	3045.9	600.6	3217.5
L Supplementary motor cortex	3517.8	900.9	2059.2
R superior parietal lobule	386.1	1415.7	429
L inferior parietal lobule	42.9	2445.3	343.2
R inferior parietal lobule	85.8	1630.2	214.5
L middle occipital gyrus	429	2488.2	471.9
Left lobule VI (Hem)	42.9	986.7	343.2
Right lobule VI (Hem)	42.9	1244.1	171.6

Table 4.6 – Regions engaged in the AssocL-AssocL condition

Anatomic location	Volume of Activation (mm <sup>3</sup> )		
	Early training	Late training	Generalization
L primary motor cortex	1673.1	429	3903.9
L primary sensory cortex	12.1	189.6	55.1
L inferior frontal gyrus	1329.9	471.9	429
R inferior frontal gyrus	2016.3	386.1	257.4
L middle frontal gyrus	2445.3	429	471.9
L Supplementary motor cortex	2273.7	686.4	343.2
R superior parietal lobule	343.2	2745.6	4375.8
L inferior parietal lobule	300.3	2187.9	3775.2
R inferior parietal lobule	429	1287	858
L middle occipital gyrus	128.7	2616.9	471.9
Left lobule VI (Hem)	171.6	772.2	3560.7
Right lobule VI (Hem)	0	1458.6	2445.3

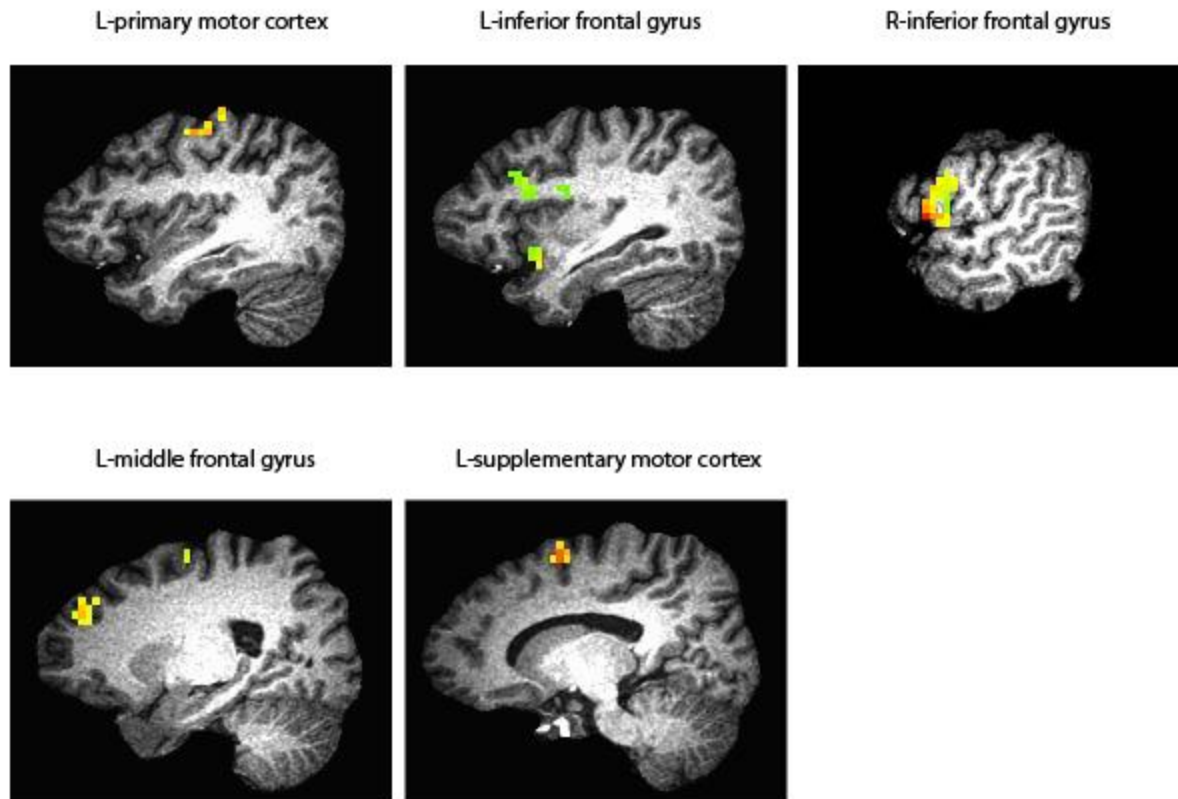


Fig. 4.6- These images present activation during the early phase of the training session. The top slices show brain activation areas in left inferior frontal gyrus, left primary motor cortex, and left middle frontal gyrus. The bottom slices present brain activation areas in left supplementary motor cortex and right inferior frontal gyrus.

#### 4.4.3 Brain activation observed during the late phase of the training session

Fig 4.7 showed brain regions that were activated during the late training phase. The main areas included right superior parietal lobule, left inferior parietal lobule, right inferior parietal lobule, left middle occipital gyrus, and bilaterally in the cerebellum (VI) .

#### **4.4.4 Brain activation during the early phase of the generalization session**

For the two subjects in the Dissoc-to-AssocL and Dissoc-to-AssocR conditions, the early phase of the generalization session was associated with the brain activation in left primary motor cortex, left middle frontal gyrus, left supplementary motor cortex (see Table 4.2, 4.3, Fig 4.8 and 4.11). For the subject in the AssocL-to-AssocL condition, it was associated with the brain activation in left primary motor cortex, right superior parietal lobule, left inferior parietal lobule, and bilaterally in the cerebellum (VI) (see Table 4.4, Fig 4.9 and 4.10). These areas were overlaid onto anatomical slices. From the results, we found that motor transfer is associated with a reduction in activity of brain regions that play an important role early in the adaptation process, including parietal lobe and cerebellum (Fig 4.10 and 4.11).

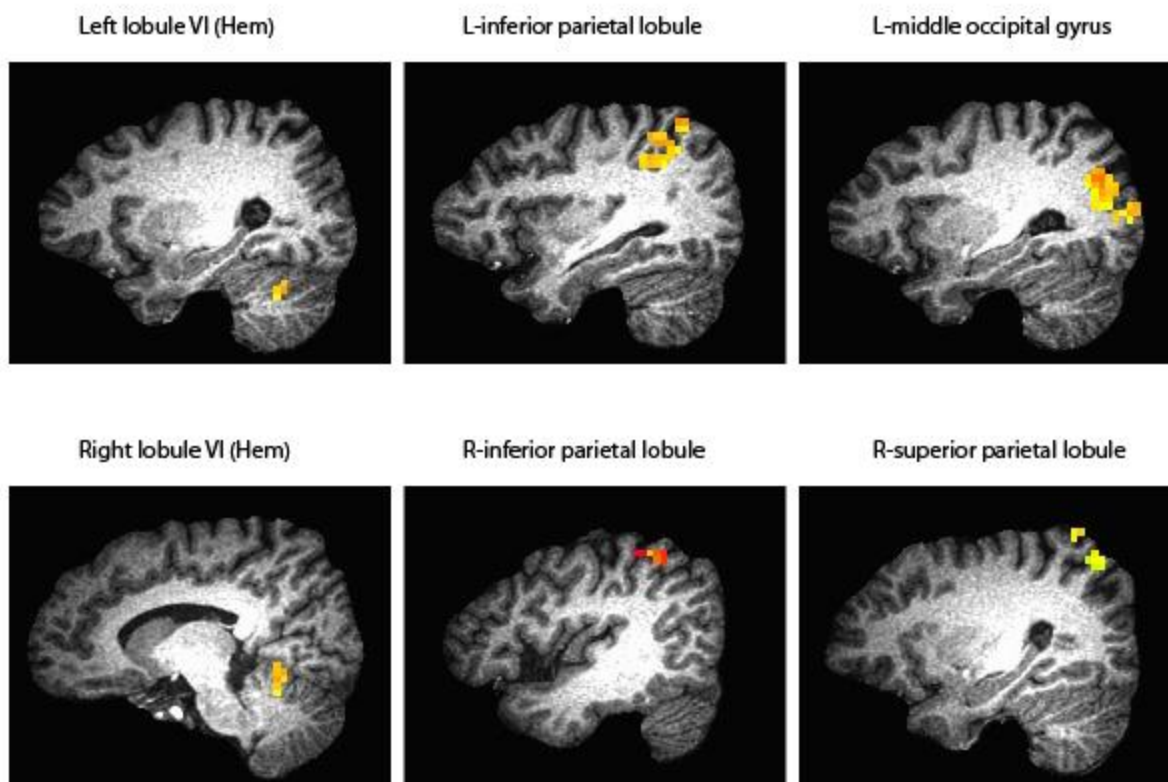


Fig. 4.7- These images present activation during the late phase of the training session. The top slices indicate brain activation areas in left lobule VI, left inferior parietal lobule and left middle occipital gyrus. The bottom slices present brain activation areas in right lobule, right inferior parietal lobule and right superior parietal lobule

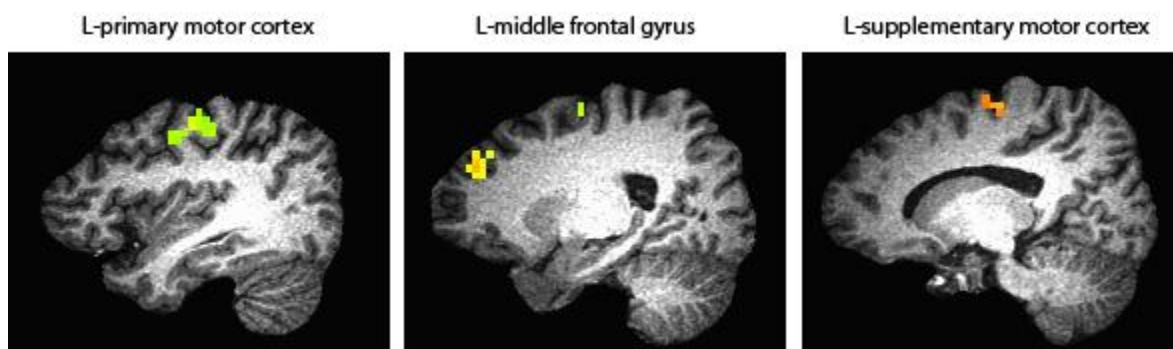


Figure. 4.8, These images present activation during the early phase of the generalization session for the Dissoc-to-AssocL and Dissoc-to-AssocR conditions, including left primary motor cortex, left middle frontal gyrus and left supplementary motor cortex.

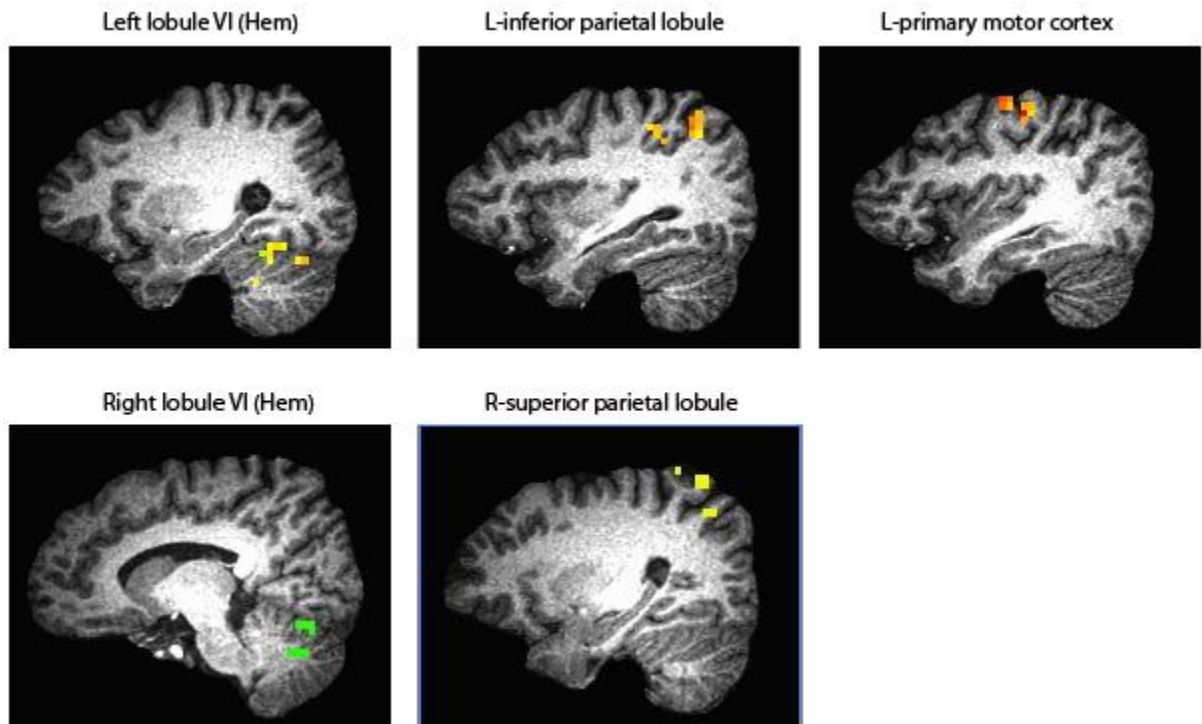


Figure. 4.9, These images present activation during the early phase of the generalization session for the AssocL-to-AssocL condition. The top slices indicate brain activation areas in left lobule VI, left primary motor cortex and left inferior parietal lobule. The bottom slices present brain activation areas in right lobule and right superior parietal lobule

## AssocL-AssocL condition

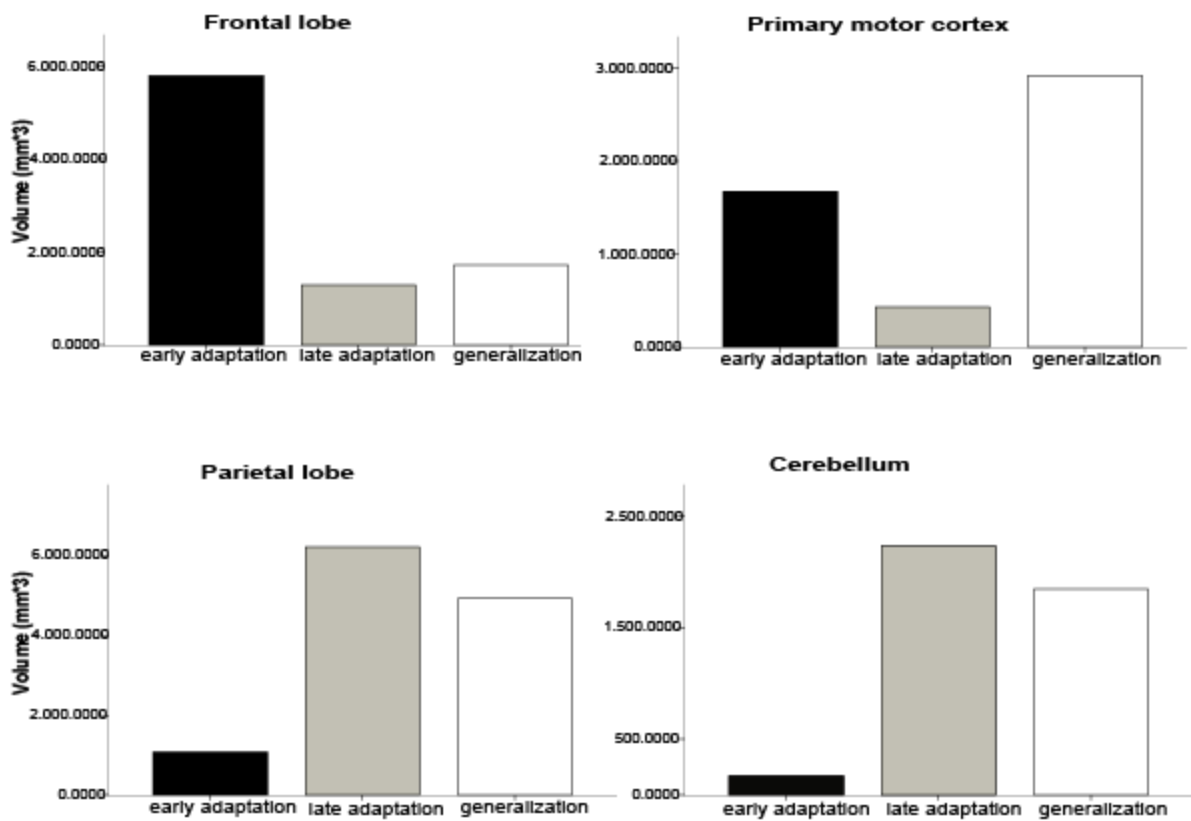


Figure 4.10, Activation patterns across the early, late phase of the training sessions and the early phase of the generalization session for the AssocL-AssocL condition.

### Dissoc-AssocL condition

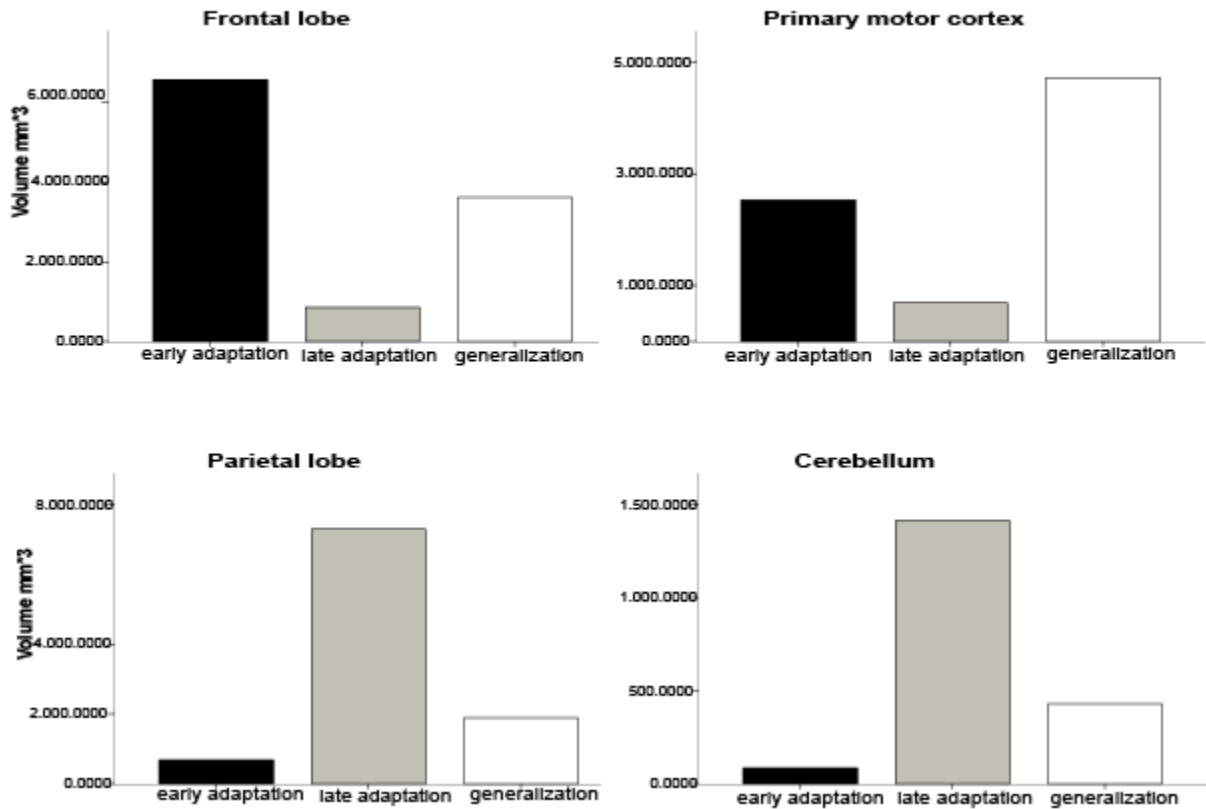


Figure 4.11, Activation patterns across the early, late phase of the training sessions and the early phase of the generalization session for the Dissoc-AssocL condition.

## 4.5 Discussion

Our behavioral study has demonstrated limited transfer across movement conditions within the same arm under the conditions in which visual and motor workspaces were separated, which support the view that a conflict between visual and proprioceptive information in terms of workspace location disrupts the development of a neural representation associated with a novel visuomotor condition. To further confirm this view, we measured fMRI activation while subjects learned a visuomotor adaptation

task with right hand in a condition in which visual and motor workspaces were dissociated, and subsequently performed the adaptation task with the same hand in a condition in which visual and motor workspace were associated. We found that left primary motor cortex, left inferior frontal gyrus, right inferior frontal gyrus, left middle frontal gyrus, left supplementary motor cortex were associated with early visuomotor adaptation, which has been found to be activated in previous visuomotor learning studies ( Ghilardi et al., 2000; Imamizu et al., 2000; Krakauer et al., 2004; Seidler et al., 2006). Right superior parietal lobule, left inferior parietal lobule, right inferior parietal lobule, left middle occipital gyrus, and the cerebellum (bilateral) showed significant activation during the late training phase. Activated regions during the early generalization phase in the subject who was tested in the AssocL-to-AssocL condition overlapped with the regions that were activated during the late training phase; and the regions activated during the early generalization phase in the subjects who were tested in the Dissoc-to-AssocL or –to-AssocR conditions overlapped with the regions that were activated during the early training phase.

It has been shown that motor adaptation involves two distinct adaptive processes. One process induces fast learning but has poor retention, whereas the other leads to slow learning but retains information well (Smith et al. 2006). Similar to the findings in that study, we found that generalization of visuomotor adaptation was associated with a reduction in activity of brain regions that were typically involved in the early adaptation (training) phase, including left inferior frontal gyrus and right inferior frontal gyrus. This makes sense because the motor memory for the early learning decays fast. Generalization of learning is thought to be correlated with the retrieval of a previously formed internal

model, allowing the learner to move more quickly, when the same task is used in both the adaptation and the generalization sessions. Thus, the brain regions activated in the early generalization phase were expected to be similar to those observed in the late adaptation phase, including right superior parietal lobule, left inferior parietal lobule, and the bilateral cerebellum (VI).

Early adaptation phase was associated with the activation of middle frontal gyrus and other regions in the frontal lobe. A recent neurophysiological study has shown that the regions in the frontal lobe, especially middle frontal gyrus, play a significant role in on-line movement corrections during visuomotor adaptation (Lee and van Donkelaar, 2006). In that study, the investigators applied transcranial magnetic stimulation (TMS) to the left dorsal premotor cortex during early adaptation, and found that the hand-paths became straight, and the rate of adaptation reduced. In contrast, TMS applied to the dorsal premotor cortex during the late adaptation did not disrupt the adaptation process, indicating that left middle frontal gyrus is associated with on-line trajectory adjustments but not motor learning. Another TMS work studied by Praeg and colleagues (2005) also suggested that PMC is not correlated with sensorimotor learning, but rather involved in movement preparation. The current study demonstrated that left middle frontal gyrus (dorsal premotor cortex) play a more important role in the early adaptation and in transfer with limited generalization, which supports the view that the left middle frontal gyrus contributes to trajectory adjustments during adaptation.

Brain activation increased in the inferior (bilateral) and superior parietal lobules during the late adaptation phase, which is not consistent with the argument made in a previous study that these regions are more important in the early phase of visuomotor

adaptation, and become less critical later during the adaptation (Graydon et al. 2005). However, Clower et al. (1996) observed the critical involvement of a transition region between the superior and inferior parietal lobules during the process of ongoing adaptation. The early generalization phase in the association condition was correlated with the activity in right superior parietal lobule, left inferior parietal lobule, and bilaterally in the cerebellum, which is thought to be related to the development of an internal model of visuomotor transformation. Therefore, it appears that the neural correlates associated with the early generalization phase overlap with those associated with the late adaptation phase (cf. Graydon et al. 2005; Imamizu et al. 2000; Seidler et al. 2008). These findings suggest that the same internal model is used during both the adaptation and the generalization processes as long as the same task (or sensorimotor condition) is employed in both processes. In addition, we found a reduction in activation in the frontal gyrus at the early adaptation phase and at the early generalization phase, which might imply that cognitive demands during the generalization process are lower than those during the adaptation (training) phase.

In some respects, our results are consistent with the findings from Muellbacher et al. (2002). In their study, they found rTMS to M1 immediately after learning interfered with retention of the motor skill during a ballistic finger movement task, which indicate that M1 is involved in early motor memory consolidation. In our study, we found there were more active in M1 at the early adaptation and at the early generalization than at the late adaptation, which identify the important role for M1 in motor memory formation of novel environment, one that is not relevant to memory stabilization.

## **4.6 Study limitations**

The major findings in this study must be interpreted with respect to several limitations: (1) we cannot make any strong arguments or conclusions based on our fMRI data due to the small sample size; (2) though the head movement was minimized using the image registration method, it could not be eliminated completely. Therefore, it might result in false recruitment in the functional images.

## **4.7 Conclusion**

We investigated fMRI activation while subjects learned a visuomotor adaptation task with their right hand in a condition in which visual and motor workspaces were either dissociated or associated with each other, and subsequently performed the same visuomotor task with the same hand in a condition in which visual and motor workspace were associated. Our main results suggest that the neural involvement is similar between the early training and the early generalization phases in the ‘dissoc-to-assoc’ conditions; while that is similar between the late adaptation and the early generalization phases in the ‘assoc-to-assoc’ condition. We propose that a conflict between visual and motor workspaces interfere with the development of a neural representation (i.e., an internal model) underlying novel visuomotor adaptation.

## **Chapter 5**

### **Conclusion and Future direction**

#### **5.1 Conclusion and Future direction**

This thesis includes two studies. In the first study, we aimed to test the effects of visual and motor workspace dissociation on the generalization of visuomotor adaptation across different conditions within the same arm during reaching movement using a robotic device. We observed that when the subjects first adapted to a visuomotor rotation under a condition in which the visual and motor workspaces were separated, the extent of generalization was much smaller than that observed in the other condition in which the two workspaces were combined. This finding indicates that the separation of visual and motor workspaces has a substantial influence on the pattern of generalization. The second study aimed to investigate the effects of dissociation between visual and motor workspace on the development of a neural representation following visuomotor adaptation using fMRI. We found that a visual-proprioceptive conflict in terms of workspace locations disrupts the development of a neural representation, or an internal model, that is associated with novel visuomotor adaptation, thus resulting in limited generalization of visuomotor adaptation.

The current findings suggest that transfer of learning occurs best in a condition in which visual and motor workspaces are physically associated with each other. In this case, transfer of learning shows brain activation patterns that appear to look like those observed in the late phase of motor learning, indicating that the same internal model is used in both the learning and the generalization conditions. Early learning process may

also be associated with transfer of learning, but concrete evidence is lacking, which requires further investigation.

In the first study, we did not observe any difference between the two dissociation groups (Dissoc-AssocM, Dissoc-AssocL), which may be attributed to the fact that we only had five subjects in each group. Including additional subjects in these groups might be needed in future studies. Only three subjects were tested in the second study, so we cannot make a conclusive assertion at this stage due to the limited sample size. Including additional subjects in the second study is also needed in future studies.

## REFERENCES

- [1] Abeele, S., & Bock, O. (2001). Sensorimotor adaptation to rotated visual input: different mechanisms for small versus large rotations. *Experimental Brain Research*, 140(4), 407-410.
- [2] Abeele, S., & Bock, O. (2001). Mechanisms for sensorimotor adaptation to rotated visual input. *Experimental Brain Research*, 139(2), 248-253.
- [3] Anguera, J. A., Russell, C. A., Noll, D. C., & Seidler, R. D. (2007). Neural correlates associated with intermanual transfer of sensorimotor adaptation. *Brain research*, 1185(1), 136-151.
- [4] Ariff, G., Donchin, O., Nanayakkara, T., & Shadmehr, R. (2002). A real-time state predictor in motor control: study of saccadic eye movements during unseen reaching movements. *The Journal of Neuroscience*, 22(17), 7721-7729.
- [5] Baraduc, P., & Wolpert, D. M. (2002). Adaptation to a visuomotor shift depends on the starting posture. *Journal of Neurophysiology*, 88(2), 973-981.
- [6] Bagesteiro LB, Sainburg RL, Handedness: dominant arm advantages in control of limb dynamics. *J. Neurophysiol.* 88 (2002) 2408–2421.
- [7] Bagesteiro LB, Sainburg RL, Nondominant arm advantages in load compensation during rapid elbow joint movements. *J. Neurophysiol.* 90 (2003) 1503–1513.
- [8] Bernier PM, Gauthier GM, Blouin J, Evidence for distinct, differentially adaptable sensorimotor transformations for reaches to visual and proprioceptive targets. *J. Neurophysiol.* 98 (2007) 1815–1819.
- [9] Bock, O., Abeele, S., & Eversheim, U. (2003). Human adaptation to rotated vision: interplay of a continuous and a discrete process. *Experimental brain research*, 152(4), 528-532.
- [10] Bock, O. (1992). Adaptation of aimed arm movements to sensorimotor discordance: evidence for direction-independent gain control. *Behavioural brain research*, 51(1), 41-50.
- [11] Brasted, P. J., & Wise, S. P. (2004). Comparison of learning- related neuronal activity in the dorsal premotor cortex and striatum. *European Journal of Neuroscience*, 19(3), 721-740.
- [12] Brinkman, C. (1981). Lesions in supplementary motor area interfere with a monkey's performance of a bimanual coordination task. *Neuroscience letters*, 27(3), 267-270.
- [13] Churchland, M. M., Byron, M. Y., Ryu, S. I., Santhanam, G., & Shenoy, K. V. (2006). Neural variability in premotor cortex provides a signature of motor preparation. *The Journal of neuroscience*, 26(14), 3697-3712.

- [14] Clower, D. M., Hoffman, J. M., Votaw, J. R., Faber, T. L., Woods, R. P., & Alexander, G. E. (1996). Role of posterior parietal cortex in the recalibration of visually guided reaching.
- [15] Cunningham, H. A., & Welch, R. B. (1994). Multiple concurrent visual-motor mappings: implications for models of adaptation. *Journal of Experimental Psychology: Human Perception and Performance*, 20(5), 987.
- [16] Evarts, E. V. (1968). Relation of pyramidal tract activity to force exerted during voluntary movement. *J Neurophysiol*, 31(1), 14-27.
- [17] Fernandez-Ruiz, J., Goltz, H. C., DeSouza, J. F., Vilis, T., & Crawford, J. D. (2007). Human parietal “reach region” primarily encodes intrinsic visual direction, not extrinsic movement direction, in a visual–motor dissociation task. *Cerebral Cortex*, 17(10), 2283-2292.
- [18] Flanagan, J. R., & Johansson, R. S. (2003). Action plans used in action observation. *Nature*, 424(6950), 769-771.
- [19] Fogassi, L., Gallese, V., Fadiga, L., Luppino, G., Matelli, M., & Rizzolatti, G. (1996). Coding of peripersonal space in inferior premotor cortex (area F4). *Journal of Neurophysiology*, 76(1), 141-157.
- [20] Franz E, Ivry R, Gazzaniga MS, Dissociation of spatial and temporal coupling in the bimanual movements of callosotomy patients. *Psychol. Sci.* 7 (1996) 306–310.
- [21] Galea, J. M., Vazquez, A., Pasricha, N., de Xivry, J. J. O., & Celnik, P. (2011). Dissociating the roles of the cerebellum and motor cortex during adaptive learning: the motor cortex retains what the cerebellum learns. *Cerebral Cortex*, 21(8), 1761-1770.
- [22] Gould, H. 3., Cusick, C. G., Pons, T. P., & Kaas, J. H. (1986). The relationship of corpus callosum connections to electrical stimulation maps of motor, supplementary motor, and the frontal eye fields in owl monkeys. *Journal of Comparative Neurology*, 247(3), 297-325.
- [23] Graziano, M. S., Yap, G. S., & Gross, C. G. (1994). Coding of visual space by premotor neurons. *SCIENCE-NEW YORK THEN WASHINGTON-*, 1054-1054.
- [24] Graziano, M. S., Reiss, L. A., & Gross, C. G. (1999). A neuronal representation of the location of nearby sounds. *Nature*, 397(6718), 428-430.
- [25] Graydon, F. X., Friston, K. J., Thomas, C. G., Brooks, V. B., & Menon, R. S. (2005). Learning-related fMRI activation associated with a rotational visuo-motor transformation. *Cognitive brain research*, 22(3), 373-383.
- [26] Hadipour-Niktarash A, Lee CK, Desmond JE, Shadmehr R. 2007. Impairment of retention but not acquisition of a visuomotor skill through time-dependent disruption of primary motor cortex. *J Neurosci.* 27:13413--13419.

- [27] Heuer H, Hegele M, Generalization of implicit and explicit adjustments to visuomotor rotations across the workspace in younger and older adults. *J. Neurophysiol.* 106 (2011) 2078-85.
- [28] Heuer, H., & Hegele, M. (2011). Generalization of implicit and explicit adjustments to visuomotor rotations across the workspace in younger and older adults. *Journal of Neurophysiology*, 106(4), 2078-2085.
- [29] Holtzman JD, Gazzaniga MS, Dual task interactions due exclusively to limits in processing resources. *Science* 218 (1982) 1325–1327.
- [30] Hocherman, S., & Wise, S. P. (1991). Effects of hand movement path on motor cortical activity in awake, behaving rhesus monkeys. *Experimental brain research*, 83(2), 285-302.
- [31] Hunter T, Sacco P, Nitsche MA, Turner DL. 2009. Modulation of internal model formation during force field-induced motor learning by anodal transcranial direct current stimulation of primary motor cortex. *J Physiol.* 587:2949--2961.
- [32] Hwang EJ, Smith MA, Shadmehr R, Dissociable effects of the implicit and explicit memory systems on learning control of reaching. *Exp. Brain Res.* 173 (2006) 425–437.
- [33] Imamizu, H., & Shimojo, S. (1995). The locus of visual-motor learning at the task or manipulator level: implications from intermanual transfer. *Journal of Experimental Psychology Human Perception and Performance*, 21, 719-719.
- [34] Imamizu, H., Miyauchi, S., Tamada, T., Sasaki, Y., Takino, R., Pütz, B., ... & Kawato, M. (2000). Human cerebellar activity reflecting an acquired internal model of a new tool. *Nature*, 403(6766), 192-195.
- [35] Inoue, K., Kawashima, R., Satoh, K., Kinomura, S., Sugiura, M., Goto, R., ... & Fukuda, H. (2000). A PET study of visuomotor learning under optical rotation. *Neuroimage*, 11(5), 505-516.
- [36] Ito, M. (2008). Control of mental activities by internal models in the cerebellum. *Nature Reviews Neuroscience*, 9(4), 304-313.
- [37] Kawato, M. (1999). Internal models for motor control and trajectory planning. *Current opinion in neurobiology*, 9(6), 718-727.
- [38] Kawato, M., Isobe, M., Maeda, Y., & Suzuki, R. (1988). Coordinates transformation and learning control for visually-guided voluntary movement with iteration: a Newton-like method in a function space. *Biological cybernetics*, 59(3), 161-177.
- [39] Kakei, S., Hoffman, D. S., & Strick, P. L. (1999). Muscle and movement representations in the primary motor cortex. *Science*, 285(5436), 2136-2139.

- [40] Kawato, M., Maeda, Y., Uno, Y., & Suzuki, R. (1990). Trajectory formation of arm movement by cascade neural network model based on minimum torque-change criterion. *Biological Cybernetics*, 62(4), 275-288.
- [41] Krakauer, J. W., Ghilardi, M. F., & Ghez, C. (1999). Independent learning of internal models for kinematic and dynamic control of reaching. *Nature neuroscience*, 2(11), 1026-1031.
- [42] Krakauer, J. W., Pine, Z. M., Ghilardi, M. F., & Ghez, C. (2000). Learning of visuomotor transformations for vectorial planning of reaching trajectories. *The Journal of Neuroscience*, 20(23), 8916-8924.
- [43] Krakauer, J. W., Mazzoni, P., Ghazizadeh, A., Ravindran, R., & Shadmehr, R. (2006). Generalization of motor learning depends on the history of prior action. *PLoS biology*, 4(10), e316.
- [44] Krakauer, J. W., Ghilardi, M. F., Mentis, M., Barnes, A., Veytsman, M., Eidelberg, D., & Ghez, C. (2004). Differential cortical and subcortical activations in learning rotations and gains for reaching: a PET study. *Journal of neurophysiology*, 91(2), 924-933.
- [45] Krakauer, J. W. (2006). Motor learning: its relevance to stroke recovery and neurorehabilitation. *Current opinion in neurology*, 19(1), 84-90.
- [46] Lee, J. H., & van Donkelaar, P. (2006). The human dorsal premotor cortex generates on-line error corrections during sensorimotor adaptation. *The Journal of neuroscience*, 26(12), 3330-3334.
- [47] Luppino, G., Matelli, M., Camarda, R. M., Gallese, V., & Rizzolatti, G. (1991). Multiple representations of body movements in mesial area 6 and the adjacent cingulate cortex: an intracortical microstimulation study in the macaque monkey. *Journal of Comparative Neurology*, 311(4), 463-482.
- [48] Matelli, M., Luppino, G., & Rizzolatti, G. (1985). Patterns of cytochrome oxidase activity in the frontal agranular cortex of the macaque monkey. *Behavioural brain research*, 18(2), 125-136.
- [49] Meier, J. D., Aflalo, T. N., Kastner, S., & Graziano, M. S. (2008). Complex organization of human primary motor cortex: a high-resolution fMRI study. *Journal of neurophysiology*, 100(4), 1800-1812.
- [50] Mehta, B., & Schaal, S. (2002). Forward models in visuomotor control. *Journal of Neurophysiology*, 88(2), 942-953.
- [51] Miall, R. C., Reckess, G. Z., & Imamizu, H. (2001). The cerebellum coordinates eye and hand tracking movements. *nature neuroscience*, 4(6), 638-644.
- [52] Moran, D. W., & Schwartz, A. B. (1999). Motor cortical representation of speed and direction during reaching. *Journal of Neurophysiology*, 82(5), 2676-2692.

- [53] Mitz, A. R., & Wise, S. P. (1987). The somatotopic organization of the supplementary motor area: intracortical microstimulation mapping. *The Journal of neuroscience*, 7(4), 1010-1021.
- [54] Muhammad, R., Wallis, J. D., & Miller, E. K. (2006). A comparison of abstract rules in the prefrontal cortex, premotor cortex, inferior temporal cortex, and striatum. *Journal of Cognitive Neuroscience*, 18(6), 974-989.
- [55] Muellbacher W, Ziemann U, Wissel J, Dang N, Kofler M, Faccini S, Boroojerdi B, Poewe W, Hallett M (2002) Early consolidation in human primary motor cortex. *Nature* 415:640–644.
- [56] Murata, A., Fadiga, L., Fogassi, L., Gallese, V., Raos, V., & Rizzolatti, G. (1997). Object representation in the ventral premotor cortex (area F5) of the monkey. *Journal of neurophysiology*, 78(4), 2226-2230.
- [57] Picard, N., & Strick, P. L. (2003). Activation of the supplementary motor area (SMA) during performance of visually guided movements. *Cerebral Cortex*, 13(9), 977-986.
- [58] Preuss, T. M., Stepniewska, I., & Kaas, J. H. (1996). Movement representation in the dorsal and ventral premotor areas of owl monkeys: a microstimulation study. *Journal of Comparative Neurology*, 371(4), 649-676.
- [59] Ramnani, N. (2006). The primate cortico-cerebellar system: anatomy and function. *Nature Reviews Neuroscience*, 7(7), 511-522.
- [60] Richardson, A. G., Overduin, S. A., Valero-Cabré, A., Padoa-Schioppa, C., Pascual-Leone, A., Bizzi, E., & Press, D. Z. (2006). Disruption of primary motor cortex before learning impairs memory of movement dynamics. *The Journal of neuroscience*, 26(48), 12466-12470.
- [61] Rizzolatti, G., Scandolara, C., Matelli, M., & Gentilucci, M. (1981). Afferent properties of periarculate neurons in macaque monkeys. II. Visual responses. *Behavioural brain research*, 2(2), 147-163.
- [62] Rosenbaum, D. A., & Chaiken, S. R. (2001). Frames of reference in perceptual-motor learning: Evidence from a blind manual positioning task. *Psychological research*, 65(2), 119-127.
- [63] Sainburg RL, Lateiner JE, Latash ML, Bagesteiro LB, Effects of altering initial position on movement direction and extent. *J. Neurophysiol.* 89 (2003) 401–415.
- [64] Sainburg, R. L., & Wang, J. (2002). Interlimb transfer of visuomotor rotations: independence of direction and final position information. *Experimental Brain Research*, 145(4), 437-447.
- [65] Scott, S. H., & Kalaska, J. F. (1995). Changes in motor cortex activity during reaching movements with similar hand paths but different arm postures. *Journal of Neurophysiology*, 73(6), 2563-2567.

- [66] Seidler, R. D. (2010). Neural correlates of motor learning, transfer of learning, and learning to learn. *Exercise and sport sciences reviews*, 38(1), 3.
- [67] Shadmehr, R., Smith, M. A., & Krakauer, J. W. (2010). Error correction, sensory prediction, and adaptation in motor control. *Annual review of neuroscience*, 33, 89-108.
- [68] Smith, M. A., Ghazizadeh, A., & Shadmehr, R. (2006). Interacting adaptive processes with different timescales underlie short-term motor learning. *PLoS biology*, 4(6), e179.
- [69] Sober SJ, Sabes PN, Multisensory integration during motor planning. *J. Neurosci.* 23 (2003) 6982–6992.
- [70] Taylor, J. A., Klemfuss, N. M., & Ivry, R. B. (2010). An explicit strategy prevails when the cerebellum fails to compute movement errors. *The Cerebellum*, 9(4), 580-586.
- [71] Thomas M, Bock O, Concurrent adaptation to four different visual rotations. *Exp. Brain Res.* 221 (2012) 85-91.
- [72] Vetter P, Goodbody SJ, Wolpert DM, Evidence for an eye-centered spherical representation of the visuomotor map. *J. Neurophysiol.* 81 (1999) 935–939.
- [73] Vindras, P., & Viviani, P. (1998). Frames of reference and control parameters in visuomanual pointing. *Journal of Experimental Psychology-Human Perception and Performance*, 24(2), 569-590.
- [74] Wang, J., & Sainburg, R. L. (2006). Interlimb transfer of visuomotor rotations depends on handedness. *Experimental Brain Research*, 175(2), 223-230.
- [75] Wang, J., & Sainburg, R. L. (2006). The symmetry of interlimb transfer depends on workspace locations. *Experimental Brain Research*, 170(4), 464-471.
- [76] Wang J, A dissociation between visual and motor workspace inhibits generalization of visuomotor adaptation across the limbs. *Exp. Brain Res.* 187 (2008) 483–490.
- [77] Wang J, Sainburg RL, Adaptation to visuomotor rotations remaps movement vectors, not final positions. *J. Neurosci.* 25 (2005) 4024–4030.
- [78] Weinrich, M., & Wise, S. P. (1982). The premotor cortex of the monkey. *The Journal of Neuroscience*, 2(9), 1329-1345.
- [79] Welch, R. B., Choe, C. S., & Heinrich, D. R. (1974). Evidence for a three-component model of prism adaptation. *Journal of experimental psychology*, 103(4), 700.
- [80] Woolley DG, Tresilian JR, Carson RG, Riek S, Dual adaptation to two opposing visuomotor rotations when each is associated with different regions of workspace. *Exp. Brain Res.* 179 (2007) 155–165.

- [81] Woolley DG, de Rugy A, Carson RG, Riek S, Visual target separation determines the extent of generalisation between opposing visuomotor rotations. *Exp. Brain Res.* 212 (2011) 213-24.

## APPENDIX

### APPENDIX A

```
#!/bin/tcsh -xef

echo "auto-generated by afni_proc.py, Wed Feb 27 16:04:41 2013"
echo "(version 3.36, October 17, 2012)"

# execute via :
# tcsh -xef proc.Liang |& tee output.proc.Liang

#auto block: setup =====
# script setup

# take note of the AFNI version
afni -ver

# check that the current AFNI version is recent enough
afni_history -check_date 8 May 2012
if ( $status ) then
    echo "*** this script requires newer AFNI binaries (than 8 May 2012)"
    echo " (consider: @update.afni.binaries -defaults)"
    exit
endif

# the user may specify a single subject to run with
if ( $#argv > 0 ) then
    set subj = $argv[1]
else
    set subj = Liang
endif

# assign output directory name
set output_dir = $subj.results

# verify that the results directory does not yet exist
if ( -d $output_dir ) then
    echo output dir "$subj.results" already exists
    exit
endif
```

```

# set list of runs
set runs = (`count -digits 2 1 1`)

# create results and stimuli directories
mkdir $output_dir
mkdir $output_dir/stimuli

# copy stim files into stimulus directory
cp /home/Yuming/Documents/fMRIData/Liang/e190/Results2/Training.1D \
  $output_dir/stimuli

# copy anatomy to results dir
3dcopy /home/Yuming/Documents/fMRIData/Liang/e190/Results2/anat_reaching+orig \
  $output_dir/anat_reaching

#auto block: tcat =====
# apply 3dTcat to copy input dsets to results dir, while
# removing the first 4 TRs
3dTcat -prefix $output_dir/pb00.$subj.r01.tcat \
  /home/Yuming/Documents/fMRIData/Liang/e190/Results2/training+orig'[4..$]'

# and make note of repetitions (TRs) per run
set tr_counts = ( 111 )

# -----
# enter the results directory (can begin processing data)
cd $output_dir

#auto block: outcount =====
# data check: compute outlier fraction for each volume
touch out.pre_ss_warn.txt
foreach run ( $runs )
  3dToutcount -automask -fraction -polort 2 -legendre \
    pb00.$subj.r$run.tcat+orig > outcount.r$run.1D

  # outliers at TR 0 might suggest pre-steady state TRs
  if ( `1deval -a outcount.r$run.1D"{0}" -expr "step(a-0.4)"` ) then
    echo "*** TR #0 outliers: possible pre-steady state TRs in run $run" \
      >> out.pre_ss_warn.txt
  endif
end

# concatenate outlier counts into a single time series
cat outcount.r*.1D > outcount_rall.1D

```

```

#tshift =====
# time shift data so all slice timing is the same
foreach run ( $runs )
    3dTshift -tzero 0 -quintic -prefix pb01.$subj.r$run.tshift \
        pb00.$subj.r$run.tcat+orig
end

#align =====
# for e2a: compute anat alignment transformation to EPI registration base
# (new anat will be intermediate, stripped, anat_reaching_strip+orig)
align_epi_anat.py -anat2epi -anat anat_reaching_strip+orig \
    -save_orig_skullstrip anat_reaching_strip -suffix _al_junk \
    -epi pb01.$subj.r01.tshift+orig -epi_base 2 \
    -volreg off -tshift off

#tlrc =====
# warp anatomy to standard space
@auto_tlrc -base TT_N27+tlrc -input anat_reaching_strip+orig -no_ss -suffix \
    NONE

#volreg =====
# align each dset to base volume, align to anat, warp to tlrc space

# verify that we have a +tlrc warp dataset
if ( ! -f anat_reaching_strip+tlrc.HEAD ) then
    echo "*** missing +tlrc warp dataset: anat_reaching_strip+tlrc.HEAD"
    exit
endif

# create an all-1 dataset to mask the extents of the warp
3dcalc -a pb01.$subj.r01.tshift+orig -expr 1 -prefix rm.epi.all1

# register and warp
foreach run ( $runs )
    # register each volume to the base
    3dvolreg -verbose -zpad 1 -base pb01.$subj.r01.tshift+orig'[2]' \
        -1Dfile dfile.r$run.1D -prefix rm.epi.volreg.r$run \
        -cubic \
        -1Dmatrix_save mat.r$run.vr.aff12.1D \
        pb01.$subj.r$run.tshift+orig

    # concatenate volreg, epi2anat and tlrc transformations
    cat_matvec -ONELINE \
        anat_reaching_strip+tlrc::WARP_DATA -I \
        anat_reaching_al_junk_mat.aff12.1D -I \
        mat.r$run.vr.aff12.1D > mat.r$run.warp.aff12.1D
end

```

```

# apply catenated xform : volreg, epi2anat and tlrc
3dAllineate -base anat_reaching_strip+tlrc \
  -input pb01.$subj.r$run.tshift+orig \
  -1Dmatrix_apply mat.r$run.warp.aff12.1D \
  -mast_dxyz 3.5 \
  -prefix rm.epi.nomask.r$run

# warp the all-1 dataset for extents masking
3dAllineate -base anat_reaching_strip+tlrc \
  -input rm.epi.all1+orig \
  -1Dmatrix_apply mat.r$run.warp.aff12.1D \
  -mast_dxyz 3.5 -final NN -quiet \
  -prefix rm.epi.1.r$run

# make an extents intersection mask of this run
3dTstat -min -prefix rm.epi.min.r$run rm.epi.1.r$run+tlrc
end

# make a single file of registration params
cat dfile.r*.1D > dfile_rall.1D

# -----
# create the extents mask: mask_epi_extents+tlrc
# (this is a mask of voxels that have valid data at every TR)
# (only 1 run, so just use 3dcopy to keep naming straight)
3dcopy rm.epi.min.r01+tlrc mask_epi_extents

# and apply the extents mask to the EPI data
# (delete any time series with missing data)
foreach run ( $runs )
  3dcalc -a rm.epi.nomask.r$run+tlrc -b mask_epi_extents+tlrc \
    -expr 'a*b' -prefix pb02.$subj.r$run.volreg
end

# create an anat_final dataset, aligned with stats
3dcopy anat_reaching_strip+tlrc anat_final.$subj

#blur =====
# blur each volume of each run
foreach run ( $runs )
  3dmerge -1blur_fwhm 4.0 -doall -prefix pb03.$subj.r$run.blur \
    pb02.$subj.r$run.volreg+tlrc
end

# mask =====

```

```

# create 'full_mask' dataset (union mask)
foreach run ( $runs )
  3dAutomask -dilate 1 -prefix rm.mask_r$run pb03.$subj.r$run.blur+tlrc
end

# only 1 run, so copy this to full_mask
3dcopy rm.mask_r01+tlrc full_mask.$subj

# ---- create subject anatomy mask, mask_anat.$subj+tlrc ----
# (resampled from tlrc anat)
3dresample -master full_mask.$subj+tlrc -input anat_reaching_strip+tlrc \
  -prefix rm.resam.anat

# convert to binary anat mask; fill gaps and holes
3dmask_tool -dilate_input 5 -5 -fill_holes -input rm.resam.anat+tlrc \
  -prefix mask_anat.$subj

# compute overlaps between anat and EPI masks
3dABoverlap -no_automask full_mask.$subj+tlrc mask_anat.$subj+tlrc \
  |& tee out.mask_overlap.txt

# ---- create group anatomy mask, mask_group+tlrc ----
# (resampled from tlrc base anat, TT_N27+tlrc)
3dresample -master full_mask.$subj+tlrc -prefix ./rm.resam.group \
  -input /home/Yuming/abin/TT_N27+tlrc

# convert to binary group mask; fill gaps and holes
3dmask_tool -dilate_input 5 -5 -fill_holes -input rm.resam.group+tlrc \
  -prefix mask_group

#=====scale
# scale each voxel time series to have a mean of 100
# (be sure no negatives creep in)
# (subject to a range of [0,200])
foreach run ( $runs )
  3dTstat -prefix rm.mean_r$run pb03.$subj.r$run.blur+tlrc
  3dcalc -a pb03.$subj.r$run.blur+tlrc -b rm.mean_r$run+tlrc \
    -c mask_anat.$subj+tlrc \
    -expr 'c * min(200, a/b*100)*step(a)*step(b)' \
    -prefix pb04.$subj.r$run.scale
end

#===== regress

# compute de-meant motion parameters (for use in regression)
1d_tool.py -infile dfile_rall.1D -set_nruns 1 \

```

```

-demean -write motion_demean.1D

# compute motion parameter derivatives (just to have)
1d_tool.py -infile dfile_all.1D -set_nruns 1 \
  -derivative -demean -write motion_deriv.1D

# create censor file motion_${subj}_censor.1D, for censoring motion
1d_tool.py -infile dfile_all.1D -set_nruns 1 \
  -show_censor_count -censor_prev_TR \
  -censor_motion 0.3 motion_${subj}

# run the regression analysis
3dDeconvolve -input pb04.${subj}.r*.scale+tlrc.HEAD \
  -mask mask_anat.${subj}+tlrc \
  -censor motion_${subj}_censor.1D \
  -polort 2 \
  -num_stimts 7 \
  -stim_times 1 stimuli/Training.1D 'BLOCK(2,1)' \
  -stim_label 1 1 \
  -stim_file 2 motion_demean.1D'[0]' -stim_base 2 -stim_label 2 roll \
  -stim_file 3 motion_demean.1D'[1]' -stim_base 3 -stim_label 3 pitch \
  -stim_file 4 motion_demean.1D'[2]' -stim_base 4 -stim_label 4 yaw \
  -stim_file 5 motion_demean.1D'[3]' -stim_base 5 -stim_label 5 dS \
  -stim_file 6 motion_demean.1D'[4]' -stim_base 6 -stim_label 6 dL \
  -stim_file 7 motion_demean.1D'[5]' -stim_base 7 -stim_label 7 dP \
  -fout -tout -x 1D X.xmat.1D -xjpeg X.jpg \
  -x 1D_uncensored X.nocensor.xmat.1D \
  -fitts fitts.${subj} \
  -errts errts.${subj} \
  -bucket stats.${subj}

# if 3dDeconvolve fails, terminate the script
if ( $status != 0 ) then
  echo '-----'
  echo '** 3dDeconvolve error, failing...'
  echo ' (consider the file 3dDeconvolve.err)'
  exit
endif

# display any large pairwise correlations from the X-matrix
1d_tool.py -show_cormat_warnings -infile X.xmat.1D |& tee out.cormat_warn.txt

# create an all_runs dataset to match the fitts, errts, etc.
3dTcat -prefix all_runs.${subj} pb04.${subj}.r*.scale+tlrc.HEAD

```

```

# create a temporal signal to noise ratio dataset
# signal: if 'scale' block, mean should be 100
# noise : compute standard deviation of errts
3dTstat -mean -prefix rm.signal.all all_runs.$subj+tlrc
3dTstat -stdev -prefix rm.noise.all errts.${subj}+tlrc
3dcalc -a rm.signal.all+tlrc \
      -b rm.noise.all+tlrc \
      -c mask_anat.$subj+tlrc \
      -expr 'c*a/b' -prefix TSNR.$subj

# create ideal files for fixed response stim types
1dcat X.nocensor.xmat.1D[3]' > ideal_1.1D

# compute sum of non-baseline regressors from the X-matrix
# (use 1d_tool.py to get list of regressor columns)
set reg_cols = `1d_tool.py -infile X.nocensor.xmat.1D -show_indices_interest`
3dTstat -sum -prefix sum_ideal.1D X.nocensor.xmat.1D"[$reg_cols]"

# also, create a stimulus-only X-matrix, for easy review
1dcat X.nocensor.xmat.1D"[$reg_cols]" > X.stim.xmat.1D

#blur estimation =====
# compute blur estimates
touch blur_est.$subj.1D # start with empty file

# -- estimate blur for each run in epits --
touch blur.epits.1D

set b0 = 0 # first index for current run
set b1 = -1 # will be last index for current run
foreach reps ( $tr_counts )
  @ b1 += $reps # last index for current run
  3dFWHMx -detrend -mask mask_anat.$subj+tlrc \
    all_runs.$subj+tlrc"[$b0..$b1]" >> blur.epits.1D
  @ b0 += $reps # first index for next run
end

# compute average blur and append
set blurs = ( `cat blur.epits.1D` )
echo average epits blurs: $blurs
echo "$blurs # epits blur estimates" >> blur_est.$subj.1D

# -- estimate blur for each run in errts --
touch blur.errts.1D

```

```

set b0 = 0 # first index for current run
set b1 = -1 # will be last index for current run
foreach reps ( $str_counts )
  @ b1 += $reps # last index for current run
  3dFWHMx -detrend -mask mask_anat.$subj+tlrc \
    errts.${subj}+tlrc["$b0..$b1"] >> blur.errts.1D
  @ b0 += $reps # first index for next run
end

# compute average blur and append
set blurs = ( `cat blur.errts.1D` )
echo average errts blurs: $blurs
echo "$blurs # errts blur estimates" >> blur_est.$subj.1D

# add 3dClustSim results as attributes to the stats dset
set fxyz = ( `tail -1 blur_est.$subj.1D` )
3dClustSim -both -NN 123 -mask mask_anat.$subj+tlrc \
  -fwhmxyz $fxyz[1-3] -prefix ClustSim
3drefit -atrstring AFNI_CLUSTSIM_MASK file:ClustSim.mask \
  -atrstring AFNI_CLUSTSIM_NN1 file:ClustSim.NN1.niml \
  -atrstring AFNI_CLUSTSIM_NN2 file:ClustSim.NN2.niml \
  -atrstring AFNI_CLUSTSIM_NN3 file:ClustSim.NN3.niml \
  stats.$subj+tlrc

#auto block: generate review scripts =====

# generate a review script for the unprocessed EPI data
gen_epi_review.py -script @epi_review.$subj \
  -dsets pb00.$subj.r*.tcat+orig.HEAD

# generate scripts to review single subject results
# (try with defaults, but do not allow bad exit status)
gen_ss_review_scripts.py -mot_limit 0.3 -exit0

#auto block: finalize =====

# remove temporary files
\rm -f rm.*

# if the basic subject review script is here, run it
# (want this to be the last text output)
if ( -e @ss_review_basic ) ./@ss_review_basic |& tee out.ss_review.$subj.txt

# return to parent directory

```

cd ..

---

```
# script generated by the command:
#
# afni_proc.py -subj_id Liang -script proc.Liang -scr_overwrite -blocks \
# tshift align tlrc volreg blur mask scale regress -copy_anat \
# /home/Yuming/Documents/fMRIData/Liang/e190/Results2/anat_reaching+orig \
# -tcat_remove_first_trs 4 -dsets \
# /home/Yuming/Documents/fMRIData/Liang/e190/Results2/training+orig.HEAD \
# -volreg_align_to third -volreg_align_e2a -volreg_tlrc_warp -mask_apply \
# anat -blur_size 4.0 -regress_stim_times \
# /home/Yuming/Documents/fMRIData/Liang/e190/Results2/Training.1D \
# -regress_stim_labels 1 -regress_basis 'BLOCK(2,1)' \
# -regress_censor_motion 0.3 -regress_make_ideal_sum sum_ideal.1D \
# -regress_est_blur_epits -regress_est_blur_errts
```

## APPENDIX B

```

Imports System.Runtime.InteropServices
Imports System.Threading
Public Class Form1
    <DllImport("InpOut32.dll", CharSet:=CharSet.Auto, EntryPoint:"Inp32")> _
    Shared Function Inp32(ByVal PortAddress As Short) As Short
    End Function

    <DllImport("InpOut32.dll", CharSet:=CharSet.Auto, EntryPoint:"Out32")> _
    Shared Sub Out32(ByVal PortAddress As Short, ByVal Data As Short)
    End Sub

    <DllImport("InpOut32.dll", CharSet:=CharSet.Auto,
EntryPoint:"IsInpOutDriverOpen")> _
    Shared Function IsInpOutDriverOpen() As UInt32
    End Function

    <DllImport("InpOutx64.dll", CharSet:=CharSet.Auto, EntryPoint:"Inp32")> _
    Shared Function Inp32_x64(ByVal PortAddress As Short) As Short
    End Function

    <DllImport("InpOutx64.dll", CharSet:=CharSet.Auto, EntryPoint:"Out32")> _
    Shared Sub Out32_x64(ByVal PortAddress As Short, ByVal Data As Short)
    End Sub

    <DllImport("InpOutx64.dll", CharSet:=CharSet.Auto,
EntryPoint:"IsInpOutDriverOpen")> _
    Shared Function IsInpOutDriverOpen_x64() As UInt32
    End Function

    Dim m_bX64 As Boolean = False
    'Dim Sequence As Integer = 0

    'Dim k As Integer = 0
    'Dim i As Integer = 0
    'Dim j As Integer = 0
    'Define pause time
    'Dim pause(0) As Integer
    'Define stimulus time
    Dim Time_Sequence(0) As Integer
    Dim stimulus_end(0) As Integer
    'Public Shared CoverForm As New Form()

```

```

Public Shared Getstart As String =
"C:\Users\Public\Documents\NeuroScript\410\scripts\start.txt"
Public Shared finishtrial As String =
"C:\Users\Public\Documents\NeuroScript\410\scripts\finish.txt"

```

```

Private Sub Button1_Click(ByVal sender As Object, ByVal e As EventArgs) Handles
Button1.Click

```

```

    Timer1.Enabled = True

```

```

    If My.Computer.FileSystem.FileExists(finishtrial) Then
        Try
            System.IO.File.Create(finishtrial).Dispose()
            System.IO.File.Delete(finishtrial)
        Catch
            System.IO.File.Create(finishtrial).Dispose()
        End Try
    End If

```

```

    Me.TopMost = True
End Sub

```

```

Private Sub Timer1_Tick(ByVal sender As System.Object, ByVal e As
System.EventArgs) Handles Timer1.Tick

```

```

    Me.TopMost = True
    Dim BaseAddress As String, RealAddress As Integer, intReadVal As Integer

```

```

    BaseAddress = ComboBox1.Text
    BaseAddress = Val("&H" & BaseAddress)
    TextBox2.Text = BaseAddress

```

```

    If CheckBox2.Checked = True Then
        RealAddress = BaseAddress + 1
    End If

```

```

    Try
        Dim iPort As Short
        iPort = RealAddress

```

```

        If (m_bX64) Then
            TextBox1.Text = Inp32_x64(iPort).ToString()
        Else

```

```

        TextBox1.Text = Inp32(iPort).ToString()
    End If

    Catch ex As Exception
        MessageBox.Show("An error occurred:\n" + ex.Message)
    End Try

    intReadVal = Convert.ToInt16(TextBox1.Text)

    If (intReadVal = 56) Then
        Form3.Hide()
        Form2.Show()
        Timer2.Enabled = True
        Timer1.Enabled = False
    End If
End Sub

Private Sub Timer2_Tick(ByVal sender As System.Object, ByVal e As
System.EventArgs) Handles Timer2.Tick

    Form2.Label1.Text = Val(Form2.Label1.Text) - 1
    Form2.Show()
    If Form2.Label1.Text = 0 Then
        Form2.Hide()
        Timer2.Enabled = False
        Timer3.Enabled = True
        stimulus_end(0) = 0
        Time_Sequence(0) = 0
    End If
End Sub

Private Sub Timer3_Tick(ByVal sender As System.Object, ByVal e As
System.EventArgs) Handles Timer3.Tick

    TextBox3.Text = Val(TextBox3.Text) + 1

    If My.Computer.FileSystem.FileExists(finishtrial) Then
        j = j + 1
        ReDim Preserve stimulus_end(j)
        stimulus_end(j) = Val(TextBox3.Text)
        Try
            System.IO.File.Create(finishtrial).Dispose()
            System.IO.File.Delete(finishtrial)
        Catch

```

```

        System.IO.File.Create(finishtrial).Dispose()
    End Try
    TextBox4.Text = Val(TextBox4.Text) + 1
End If

If ComboBox2.Text.Contains("Baseline") Then
    If Val(TextBox4.Text) = 40 Then
        Timer3.Enabled = False
    End If
End If

If ComboBox2.Text.Contains("Generalization") Then
    If Val(TextBox4.Text) = 40 Then
        Timer3.Enabled = False
    End If
End If

If ComboBox2.Text.Contains("Training") Then
    If Val(TextBox4.Text) = 80 Then
        Timer3.Enabled = False
    End If
End If
End Sub

Private Sub Button2_Click(ByVal sender As System.Object, ByVal e As
System.EventArgs) Handles Button2.Click

    For i As Integer = 1 To j
        ReDim Preserve Time_Sequence(i)
        Time_Sequence(i) = stimulus_end(i) - stimulus_end(i - 1)
    Next

    System.IO.File.WriteAllLines("C:\Users\ylei\Desktop\Sequence_(session)_(subject).txt",
Array.ConvertAll(Time_Sequence, New Converter(Of Integer, String)(Function(t As
Integer) t.ToString())))

End Sub

Private Sub Button3_Click(ByVal sender As System.Object, ByVal e As
System.EventArgs) Handles Button3.Click
    Me.WindowState = FormWindowState.Minimized
    Form3.Show()
    Form3.TopMost = True
End Sub
End Class

```

```

Imports System.Runtime.InteropServices
Imports System.Threading
Public Class Form1
    <DllImport("InpOut32.dll", CharSet:=CharSet.Auto, EntryPoint:="Inp32")> _
    Shared Function Inp32(ByVal PortAddress As Short) As Short
    End Function

    <DllImport("InpOut32.dll", CharSet:=CharSet.Auto, EntryPoint:="Out32")> _
    Shared Sub Out32(ByVal PortAddress As Short, ByVal Data As Short)
    End Sub

    <DllImport("InpOut32.dll", CharSet:=CharSet.Auto,
EntryPoint:="IsInpOutDriverOpen")> _
    Shared Function IsInpOutDriverOpen() As UInt32
    End Function

    <DllImport("InpOutx64.dll", CharSet:=CharSet.Auto, EntryPoint:="Inp32")> _
    Shared Function Inp32_x64(ByVal PortAddress As Short) As Short
    End Function

    <DllImport("InpOutx64.dll", CharSet:=CharSet.Auto, EntryPoint:="Out32")> _
    Shared Sub Out32_x64(ByVal PortAddress As Short, ByVal Data As Short)
    End Sub

    <DllImport("InpOutx64.dll", CharSet:=CharSet.Auto,
EntryPoint:="IsInpOutDriverOpen")> _
    Shared Function IsInpOutDriverOpen_x64() As UInt32
    End Function

    Dim m_bX64 As Boolean = False
    'Dim Sequence As Integer = 0

    'Dim k As Integer = 0
    Dim i As Integer = 0
    Dim j As Integer = 0
    'Define pause time
    'Dim pause(0) As Integer
    'Define stimulus time
    Dim Time_Sequence(0) As Integer
    Dim stimulus_end(0) As Integer
    Public Shared CoverForm As New Form()
    Public Shared Getstart As String =
"C:\Users\Public\Documents\NeuroScript\410\scripts\start.txt"

```

```
Public Shared finishtrial As String =
"C:\Users\Public\Documents\NeuroScript\410\scripts\finish.txt"
```

```
Private Sub Button1_Click(ByVal sender As Object, ByVal e As EventArgs) Handles
Button1.Click
```

```
    Timer1.Enabled = True
```

```
    If My.Computer.FileSystem.FileExists(finishtrial) Then
```

```
        Try
```

```
            System.IO.File.Create(finishtrial).Dispose()
```

```
            System.IO.File.Delete(finishtrial)
```

```
        Catch
```

```
            System.IO.File.Create(finishtrial).Dispose()
```

```
        End Try
```

```
    End If
```

```
    Me.TopMost = True
```

```
End Sub
```

```
Private Sub Timer1_Tick(ByVal sender As System.Object, ByVal e As
System.EventArgs) Handles Timer1.Tick
```

```
    Me.TopMost = True
```

```
    Dim BaseAddress As String, RealAddress As Integer, intReadVal As Integer
```

```
    BaseAddress = ComboBox1.Text
```

```
    BaseAddress = Val("&H" & BaseAddress)
```

```
    TextBox2.Text = BaseAddress
```

```
    If CheckBox2.Checked = True Then
```

```
        RealAddress = BaseAddress + 1
```

```
    End If
```

```
    Try
```

```
        Dim iPort As Short
```

```
        iPort = RealAddress
```

```
        If (m_bX64) Then
```

```
            TextBox1.Text = Inp32_x64(iPort).ToString()
```

```
        Else
```

```
            TextBox1.Text = Inp32(iPort).ToString()
```

```
        End If
```

```

Catch ex As Exception
    MessageBox.Show("An error occured:\n" + ex.Message)
End Try

```

```

intReadVal = Convert.ToInt16(TextBox1.Text)

```

```

If (intReadVal = 56) Then
    Form3.Hide()
    Form2.Show()
    Timer2.Enabled = True
    Timer1.Enabled = False
End If
End Sub

```

```

Private Sub Timer2_Tick(ByVal sender As System.Object, ByVal e As
System.EventArgs) Handles Timer2.Tick

```

```

    Form2.Label1.Text = Val(Form2.Label1.Text) - 1
    Form2.Show()
    If Form2.Label1.Text = 0 Then
        Form2.Hide()
        Timer2.Enabled = False
        Timer3.Enabled = True
        stimulus_end(0) = 0
        Time_Sequence(0) = 0
    End If
End Sub

```

```

Private Sub Timer3_Tick(ByVal sender As System.Object, ByVal e As
System.EventArgs) Handles Timer3.Tick

```

```

    TextBox3.Text = Val(TextBox3.Text) + 1

```

```

If My.Computer.FileSystem.FileExists(finishtrial) Then
    j = j + 1
    ReDim Preserve stimulus_end(j)
    stimulus_end(j) = Val(TextBox3.Text)
    Try
        System.IO.File.Create(finishtrial).Dispose()
        System.IO.File.Delete(finishtrial)
    Catch
        System.IO.File.Create(finishtrial).Dispose()
    End Try

```

```

    TextBox4.Text = Val(TextBox4.Text) + 1
End If

If ComboBox2.Text.Contains("Baseline") Then
    If Val(TextBox4.Text) = 40 Then
        Timer3.Enabled = False
    End If
End If

If ComboBox2.Text.Contains("Generalization") Then
    If Val(TextBox4.Text) = 40 Then
        Timer3.Enabled = False
    End If
End If

If ComboBox2.Text.Contains("Training") Then
    If Val(TextBox4.Text) = 80 Then
        Timer3.Enabled = False
    End If
End If
End Sub

Private Sub Button2_Click(ByVal sender As System.Object, ByVal e As
System.EventArgs) Handles Button2.Click

    For i As Integer = 1 To j
        ReDim Preserve Time_Sequence(i)
        Time_Sequence(i) = stimulus_end(i) - stimulus_end(i - 1)
    Next

    System.IO.File.WriteAllLines("C:\Users\ylei\Desktop\Sequence_(session)_(subject).txt",
Array.ConvertAll(Time_Sequence, New Converter(Of Integer, String)(Function(t As
Integer) t.ToString()))

End Sub

Private Sub Button3_Click(ByVal sender As System.Object, ByVal e As
System.EventArgs) Handles Button3.Click
    Me.WindowState = FormWindowState.Minimized
    Form3.Show()
    Form3.TopMost = True
End Sub
End Class

```

## APPENDIX C

### Equipment Checklist:

**Laptop PC**

**Parallel Port Card**

**Joystick** (2 components)

**BNC cable**

**VGA cable**

**fMRI documents:** Consent form/ IRB approval letter/ fMRI data log sheet/ scanner\_patient\_setup/ Task setup procedures (Mock and Scanner);

### Mock Scanning Procedures Checklist:

#### **To Set Up the Joystick:**

Insert Parallel Port Card into our laptop;

Connect the joystick USB end to our laptop PC;

Connect trigger box to our laptop PC;

Connect the projector to our laptop PC w/ the VGA cable; and press the button to reverse image.

#### **To Run the Experiment:**

1. Open “ParallelPortReading” on the desktop. Click “Start” Button

2. Open MovAlyzeR and select the experiment that will be run.

- Only 1 experiment w/n each subject for Mock Baseline session.

3. Read instructions (first check if the subject can hear you loud and clear, then read the following):

*“You will see a statement on the screen, which reads “Please Wait” very soon. When statement disappears, you will see 20 seconds countdown on the screen; the task gets*

*start after countdown. Once task starts, Long press the mouse and make sure controller is activated, and please bring the cursor inside the red circle displayed in the center of the screen, and wait until a target appears. Once the target appears, please bring the cursor to the target rapidly, and as straight as possible. Do not make any corrections after you made your initial reaching movement. Once the target disappears, please bring the cursor back to the red circle displayed in the screen center, and wait for the next target.”*

4. Get the MovAlyzeR task started.

5. Click “Wait Trigger” button in the “ParallelPortReading” app. A picture with words “Please Wait” should show up, indicating that the task is ready to begin.

When trigger arrives, the words “Please Wait” should disappear; subject will see 20 seconds countdown and the task should begin.

Once the experiment ends, close current program.

Continue with the next experiment (go back to step 1).

## Experimental Procedures Checklist:

### To Set Up the Joystick

Insert Parallel Port Card into our laptop;

Connect trigger box to our laptop PC;

Connect the joystick USB end to our laptop PC; connect the VGA end to the control panel connector 7.

Connect speakers or audio output to headphone jack of laptop; and check with the scanner operator to ensure volume is set ok for the subject.

Connect the projector to our laptop PC w/ the VGA cable.

### To Run the Experiment:

1. Open “ParallelPortReading” on the desktop; Click “Start” button.
2. Open MovAlyzeR and select the experiment that will be run.
  - 3 different experiments w/n each subject for Baseline, Training, Generalization sessions.
  - Data should be saved in the file named as subject’s name.
3. Read instructions (first check if the subject can hear you loud and clear, then read the following):

*“You will see a statement on the screen, which reads “Please Wait” very soon. When statement disappears, you will see 20 seconds countdown on the screen; the task gets start after countdown. Once task starts, Long press the mouse and make sure controller is activated, and please bring the cursor inside the red circle displayed in the center of the screen, and wait until a target appears. Once the target appears, please bring the cursor to the target rapidly, and as straight as possible. Do not make any corrections after you made your initial reaching movement. Once the target disappears, please bring the cursor back to the red circle displayed in the screen center, and wait for the next target.”*

Get the MovAlyzeR task started.

- Confirm with the scanner operator that you are ready to start the scan.

- Once the scanning starts, make sure the program is automatically triggered.
- Make sure (1) the time trigger hasn't been triggered, and (2) the scanner operator have finished the pre-scan.

When operator is ready to start the scan, we click "Wait Trigger" button to start task. Then plug Joystick USB into laptop.

- . Click "Wait Trigger" button in the "ParallelPortReading" app. A picture with words "Please Wait" should show up, indicating that the task is ready to begin.

When trigger arrives, the words "Please Wait" should disappear; subject will see 20 seconds countdown and the task should begin.

Once the experiment ends, close current program; **click "Time Sequence" button in program to save Time\_Sequence.txt file into subject fold**

Continue with the next experiment (go back to step 1).

## APPENDIX D

## fMRI data processing flow chart

